

The landscape of intersecting brane models

Michael R. Douglas^{1,&} and Washington Taylor^{2,3}

¹*NHETC and Department of Physics and Astronomy
Rutgers University
Piscataway, NJ 08855-0849, USA*

²*Center for Theoretical Physics
MIT
Cambridge, MA 02139, USA*

³*Department of Physics
Stanford University
Stanford, CA 94305-4060, USA*

& I.H.E.S., Le Bois-Marie, Bures-sur-Yvette, 91440 France

mrd@physics.rutgers.edu, wati at mit.edu

ABSTRACT: We develop tools for analyzing the space of intersecting brane models. We apply these tools to a particular T^6/\mathbb{Z}_2^2 orientifold which has been used for model building. We prove that there are a finite number of intersecting brane models on this orientifold which satisfy the Diophantine equations coming from supersymmetry. We give estimates for numbers of models with specific gauge groups, which we confirm numerically. We analyze the distributions and correlations of intersection numbers which characterize the numbers of generations of chiral fermions, and show that intersection numbers are roughly independent, with a characteristic distribution which is peaked around 0 and in which integers with fewer divisors are mildly suppressed.

As an application, the number of models containing a gauge group $SU(3) \times SU(2) \times U(1)$ or $SU(4) \times SU(2) \times SU(2)$ and 3 generations of appropriate types of chiral matter is estimated to be order $\mathcal{O}(10)$, in accord with previous explicit constructions. As another application of the methods developed in the paper, we construct a new pair of 3-generation $SU(4) \times SU(2) \times SU(2)$ Pati-Salam models using intersecting branes.

We conclude with a description of how this analysis can be generalized to a broader class of Calabi-Yau orientifolds, and a discussion of how the numbers of IBM's are related to numbers of stabilized vacua.

Contents

1. Introduction	2
2. Models on the torus with fixed gauge group	5
2.1 Supersymmetric branes on the toroidal orientifold	6
2.2 Types of branes	8
2.3 Symmetries	9
2.4 Proof of finiteness	9
2.5 Estimates	12
2.5.1 One-stack models	13
2.5.2 Two brane stacks	17
2.5.3 Three stacks	23
2.5.4 Hidden sector A -type branes	25
2.6 Summary of results	25
2.7 Algorithms	26
3. Distribution of intersection numbers	28
3.1 Single intersection numbers	29
3.2 Multiple intersection numbers	34
4. Some specific models	36
5. More general Calabi-Yau orientifolds	39
5.1 General framework	40
5.1.1 Basic definitions	40
5.1.2 Calabi-Yau geometric data	41
5.1.3 Matter content	44
5.2 Examples	44
5.2.1 Torus	44
5.2.2 Elliptically fibered Calabi-Yau manifolds	46
5.2.3 Toric hypersurface Calabi-Yau manifolds	47
5.3 Positivity and brane classes	47
5.4 Rough estimate of number of configurations	49
6. Relevance for the problem of counting more general vacua	50
7. Conclusions	52

1. Introduction

Intersecting brane models (IBM's) have been widely studied in recent years as quasi-realistic compactifications of superstring theory [9]. One reason for their popularity is that they appear to contain all of the necessary ingredients – the Standard Model, additional gauge sectors to provide supersymmetry breaking, and the possibility of stabilizing moduli by fluxes and other means – without requiring sophisticated mathematics to analyze.

In this work, we carry out a systematic analysis of a simple class of models of this type, namely intersecting brane models on type IIB orientifolds of $T^6/\mathbb{Z}_2 \times \mathbb{Z}_2$. We begin with some brief comments regarding the purpose of explicit constructions of string vacua, after which we will describe in more detail the approach taken in this paper.

The primary goals in the study of string compactifications at present are:

1. To find models which reproduce all physics observed experimentally to date, and to work out the predictions of these models for future observations.
2. To discover new physical mechanisms which might have observable signatures, or might solve theoretical problems.
3. To get an overall picture of the set of all “interesting” models, and to find structure in this set which might help in making predictions, or in uncovering deeper formal structures in string/M theory.

These are complementary goals, each with strengths and weaknesses. We note that we have no reason to think that the straightforward approach of (1) will lead to a unique candidate vacuum, nor that any particular mechanism found in (2) will be realized in our physical vacuum; on the other hand (3) is at present a complicated problem which must be simplified to make progress, running the risk of missing important features of the physics. In any case it seems to us that all three goals are essential to any clear understanding of the implications and testability of string theory.

While the methods we develop in this paper may be useful in explicit model building as in (1), our primary interest here is more in (3). We are interested in IBM's as a simple calculable ensemble of vacua realizing a large variety of gauge groups and matter contents, in which we can study the distribution of various physical features. We follow the point of view advocated in [36], where the problem of counting isolated (or “stabilized”) vacua was set out in a precise way. This work also suggested as a simple Ansatz that various observables, in particular intersection numbers between pairs of branes, might be independent in ensembles of vacua coming from string theory, and this idea was used to estimate the fraction of IBM's realizing the Standard Model gauge group and matter representations as somewhere between 10^{-10} and 10^{-20} .

In recent works of the Munich group [8, 40] this type of question has been analyzed in detail in the $T^6/\mathbb{Z}_2 \times \mathbb{Z}_2$ orientifold. They performed an automated scan over supersymmetric brane configurations satisfying the tadpole conditions, and obtained statistics for the resulting ensemble of models. As we will review, this is essentially a partition problem involving finding all subsets of a fixed set of vectors which sum to a desired vector. Such

problems are typically NP-complete, so that (for general reasons explained in [26]) it is unclear that any algorithm can do this much faster than an exhaustive search through a list of candidate models. This requires time which grows faster than any power of the numbers controlling the size of the problem (Betti numbers and the numbers entering the tadpole conditions), and indeed the computer search of [8] ran for about a year.

Now as long as the properties one is searching for are not too rare, this type of intractability can be dealt with by taking a random sample of the total ensemble, and making statistical statements based on this sample. But to interpret such results, it is important to have a precise definition of the set being sampled, and an unbiased sample. It is not entirely clear to us whether this is true of the algorithms used in [8, 40], for reasons explained in those works and which will review below.

Nevertheless, their analysis led to some interesting observations on the set of models. In particular, they found that features of the intersecting brane model field theory, such as having a $U(N)$ subgroup or a fixed number of generations of chiral fermions in a particular matter sector, were largely statistically independent. Combining the probabilities for the gauge group and number of generations of matter fields, in [40], the hypothesis of independence was used to estimate the fraction of 3 generation Standard Models to be 10^{-9} (or “one in a billion”) in this ensemble.

In this paper, we primarily study the same ensemble of intersecting brane models as in [8, 40]. Compared to these works, there are a number of differences in our approach. Perhaps the main one is that we have developed algorithms which can in principle enumerate **all** configurations of a specified type, by searching through a finite set of possibilities. The main new ingredients which enable us to do this are an analytic proof that the relevant brane configurations are finite in number, and *a priori* bounds on the homology classes of the branes which can appear.

This is not to say that one can usually do a complete enumeration in practice. For the toroidal examples we consider in detail here, this may be possible, as the number of models is of order 10^{10} . However, most ensembles on more general Calabi-Yau manifolds will have many more configurations. Still, there are good reasons to want algorithms which can generate the complete ensemble, such as to be able to do unbiased random sampling.

Another difference between this work and [8, 40] is that we focus more closely on enumerating IBM’s which contain a specified “visible” gauge group and charged matter content, leaving the rest of the model unconstrained (as was done in [31]). We then analyze the structure of the problem within this sector which leads to a specific dependence of the number of models on the gauge group and matter content. This allows searching for Standard Models, and also for other desired structure such as particular supersymmetry breaking gauge theories. It also makes the problem far more tractable computationally. While the total number of intersecting brane models grows exponentially in a tadpole parameter, the number of models with fixed gauge groups grows only polynomially. Of course, to enumerate all models, one still needs to consider all possibilities; we leave the question of whether the scan over hidden sectors can be bypassed by estimating their multiplicities for subsequent work.

A final difference is that we have not gone as far in the detailed construction of Standard

Models as [31, 40], for example leaving explicit enumeration of “tilted tori” configurations for future work. Rather, besides methodological improvements, we concentrate on getting detailed analytical and numerical estimates. We find estimates for the number of models as a function of the gauge group. We find that the number of models with a gauge group factor $U(N)$ goes as an inverse power of N . We also investigate intersection numbers between branes, which govern the number of matter fields.

The overall picture which emerges from this analysis is that for this particular orientifold, there are a calculable set of intersecting brane models which include a wide range of specified gauge groups and number of generations of chiral matter fields. For the standard model gauge group and 3 generations, the number of models is on the order of 10. Aside from the suppression of large generations for large gauge groups, and some mild number-theoretic enhancement of composite intersection numbers which seems rather model dependent, there does not seem to be any strong correlation between the specific features of the gauge group and matter content. Rather, this class of models seems naturally to give rise to an ensemble of string vacua with different gauge groups and different numbers of generations of matter fields reasonably equally distributed. Our results so far have also not confirmed the interesting claim of [40] that 3 generations (compared to 1, 2 or 4) is disfavored in this ensemble, but it may be that we did not get far enough to see this and that it might come out of a more complete analysis, for example including tilted tori.

It is important to note that just because a model class does not “explain” or prefer the correct number of generations is not a strong argument against it. An arguably better application of the statistics of vacua is to consider only vacua which fit the known data (the Standard Model) and then look at the distribution of predictions among these. Interesting predictions which can be made from IBM’s include additional charged matter, particularly with exotic gauge quantum numbers, the presence of additional gauge sectors loosely coupled to the SM (which might be useful for supersymmetry breaking), and hidden sectors (with purely gravitational coupling to the SM). All of these features appear generic, and it would be very useful to know what constraints these additional matter sectors obey. To study these issues it is important to have a wider class of semi-realistic models containing at least the standard model gauge group and the physical number of generations. Towards this end, we include here some discussion of how the analysis of this paper might be generalized to a broader class of Calabi-Yau manifolds, where we might find many more of these semi-realistic models with which to perform further analysis.

The structure of this paper is as follows: In Section 2 we study intersecting brane models on a specific toroidal orientifold with fixed gauge group. We prove that there are a finite number of SUSY models with fixed tadpoles and any fixed number of brane stacks. We develop analytic estimates of the numbers of such models, which we check using numerical experiment. We develop polynomial time algorithms for generating all models with a fixed gauge group. In Section 3 we consider the intersection numbers between brane stacks, which describe the numbers of families of matter fields associated with strings connecting the branes. We look at the distribution of intersection numbers in some generic classes of models, and analyze the statistical properties of these distributions. In Section 4 we discuss the application of our general analysis to more explicit model building, and

identify a pair of new intersecting brane models containing the standard model gauge group and 3 generations of chiral matter. In Section 5 we discuss the generalization of type II intersecting brane models to a general Calabi-Yau manifold. A similar discussion appears in [11].

One issue which we do not address in this paper is the problem of including fluxes or other effects which stabilize the moduli. The intersecting brane models we consider are only isolated points in a larger open string moduli space of supersymmetric brane configurations. In general, moving out into this moduli space corresponds to recombination of branes as well as variation of their world-volume gauge fields. A full analysis requires understanding these moduli spaces, and then stabilization of these moduli. While papers such as [13, 51] have begun to address this question by constructing intersecting brane models including NS-NS and R-R fluxes, a systematic and global approach to this problem is still lacking. In section 6, we outline a simple argument which suggests that the number of IBM's (of a slightly more general type than we consider) could be a good estimate for the number of stabilized vacua which would come out of such a full analysis. Again, we leave detailed exploration of this idea for future work.

Our conclusions appear in section 7.

2. Models on the torus with fixed gauge group

Given a particular Calabi-Yau and orientifold, there are many brane configurations which preserve supersymmetry. In this paper we consider a simplification of the full classification problem for intersecting brane models. We assume that the gauge group is chosen as an input, and we consider the problem of generating all SUSY intersecting brane models with the desired gauge group. The gauge group can either be chosen to completely saturate the tadpole, in which case there are no further hidden sectors of the theory, or the gauge group can be chosen to undersaturate the tadpole, leaving room for further “hidden” parts of the gauge group which would produce the remaining contribution needed for the tadpole. In our discussion we use the phrase “hidden” sector to describe the part of the model which does not include our gauge group of interest. We do not get into the details of phenomenology which would be needed to make one part of the gauge group visible in the low-energy theory.

After some initial discussion of supersymmetric branes on the toroidal orientifold in 2.1, 2.2, in subsection 2.3 we briefly discuss useful symmetries of the problem. We then begin the substantive analysis in subsection 2.4 by demonstrating that there are a finite number of distinct solutions to the SUSY equations containing any fixed gauge group. In subsection 2.5 we give estimates for the numbers of brane configurations with certain properties; the results of this somewhat detailed analysis are summarized in subsection 2.6. In subsection 2.7 we give efficient algorithms for generating all SUSY brane models with a fixed tadpole and fixed gauge group.

Compared to previous work, there are two essential new ingredients in our analysis and algorithms. The first new ingredient comes from the proof of finiteness, which allows us to compute explicit bounds on the range of winding numbers of the branes which can

appear. These bounds not only allow us to demonstrate that a given set of solutions is complete, but also allow us to efficiently scan the space of allowed configurations. The second new ingredient is to enumerate brane configurations independently of the Kähler moduli, and then check for each configuration whether it is supersymmetric for some value of the moduli; this avoids a time-consuming scan over moduli.

As we will show, the number of configurations with a fixed gauge group grows polynomially in the total tadpole number, with a power growing with the number of “brane stacks” or factors in the gauge group. The search algorithms typically take time which is comparable to the number of configurations; in other words one needs to search through a number of candidates comparable to the number of solutions. This is essentially the same level of difficulty as for finding flux vacua, in which the time also scales with the number of configurations. For example, for IIB flux vacua on a Calabi-Yau with third Betti number b_3 and D3 tadpole L , the number of vacua grows as $(2\pi L)^{b_3}/(b_3)!$ (for $L \gg b_3$) [2, 37], and there is probably no algorithm for finding the interesting ones which is much more efficient than exhaustive search through a large set of candidates. This number of flux vacua grows polynomially with a tadpole constraint, while it grows exponentially with the number of cycles b_3 . The exponential complexity of the general brane problem, on the other hand, arises from the need to sum over all gauge groups and thus all partitions. While we avoid this particular exponential complexity using the methods of this paper, it is distinct from that which would appear on a more general Calabi-Yau with large Betti numbers b_i , where again the number of vacua would grow exponentially in b_i . We discuss this issue further in Section 5.

As we will now describe in more detail, the problem of enumerating all intersecting brane constructions with a fixed gauge group is a polynomial time problem, while counting and characterizing the possible hidden sectors is in general exponential. However, we should emphasize that in the T^6/\mathbb{Z}_2^2 model, the full range of possible hidden sectors should also be computable due to the size of the numbers involved using the more efficient algorithms we develop here.

2.1 Supersymmetric branes on the toroidal orientifold

In this subsection we quickly review the problem of finding supersymmetric brane configurations in the T^6/\mathbb{Z}_2^2 orientifold. We follow most closely the discussion in [8], but equally good accounts include [19, 9]. Readers unfamiliar with this problem can also skip ahead to section 5, where the general setup is reviewed.

Considering T^6 as a product of 3 T^2 's with complex coordinates z_i , the \mathbb{Z}_2 actions are given by $(z_1, z_2, z_3) \rightarrow (-z_1, -z_2, z_3)$ and $(z_1, z_2, z_3) \rightarrow (z_1, -z_2, -z_3)$, while the orientifold action takes $\Omega : z_i \rightarrow \bar{z}_i$. For the subset of branes we consider, mirror symmetry is very simple (it amounts to a triple T -duality), and the IIA and IIB descriptions are equivalent. We are going to use a mixed IIA–IIB language, because while the pictures are simpler in the IIA language with wrapped D6-branes, much of the underlying mathematics and the generalization to other Calabi-Yau orientifolds can be described most easily in the IIB language.

In IIA language, the supersymmetric branes we consider are D6-branes wrapping flat T^3 submanifolds of T^6 . Such a submanifold can be described by a vector of six winding numbers n_i and m_i with $i \in \{1, 2, 3\}$, defining an embedding from a T^3 with coordinates $\sigma_1, \sigma_2, \sigma_3$ to T^6 with coordinates (X^i, Y^i) as

$$X^i = n_i \sigma_i; \quad Y^i = m_i \sigma_i.$$

To get a one-to-one embedding, the pair of winding numbers (n_i, m_i) must be relatively prime for each $i \in \{1, 2, 3\}$; such a vector is referred to as “primitive.” One can check that any such submanifold is invariant under the orbifold action \mathbb{Z}_2^2 . The orientifold Ω will act as $(n_i, m_i) \rightarrow (n_i, -m_i)$, so a consistent brane configuration is a set of branes which is invariant under Ω .

The mirror symmetry to IIB operates by T-dualizing the three coordinates Y^i . The mirror of such a brane then depends on the indices n_i . If all are non-zero, one gets a D9-brane carrying magnetic flux determined by the indices m_i . When any n_i are zero, one gets lower dimensional wrapped branes. For now, we use IIA notation; the relationship between these pictures is discussed further in Section 5.

A supersymmetric brane model consists of a set of brane stacks satisfying a common supersymmetry condition. Each brane stack is parameterized by the number of branes N and a set of winding numbers $n_i, m_i, i \in \{1, 2, 3\}$. The real part of the supersymmetry condition is

$$0 = m_1 m_2 m_3 - m_1 j_2 n_2 j_3 n_3 - m_2 j_3 n_3 j_1 n_1 - m_3 j_1 n_1 j_2 n_2. \quad (2.1)$$

Here, $j_i > 0$ are the Kähler moduli in the IIB picture, T-dual to complex structure moduli in the intersecting brane IIA picture. Each brane stack has an image under Ω where $n'_i = n_i, m'_i = -m_i$.

Using a to index the distinct brane stacks, not counting images under Ω , and denoting by $T = 8$ the bound on the total tadpoles arising from the orientifold, the tadpole conditions can be written as

$$\sum_a P_a = \sum_a Q_a = \sum_a R_a = \sum_a S_a = T \quad (2.2)$$

where the individual tadpole contributions from each brane stack are given by

$$\begin{aligned} P &= n_1 n_2 n_3 \\ Q &= -n_1 m_2 m_3 \\ R &= -m_1 n_2 m_3 \\ S &= -m_1 m_2 n_3. \end{aligned} \quad (2.3)$$

With this notation, when all tadpoles are nonvanishing the real part of the SUSY condition becomes

$$\frac{1}{P} + \frac{j}{Q} + \frac{k}{R} + \frac{l}{S} = 0. \quad (2.4)$$

where we denote $j = j_2 j_3, k = j_1 j_3, l = j_1 j_2$. The positivity part of the SUSY condition becomes

$$P + \frac{1}{j}Q + \frac{1}{k}R + \frac{1}{l}S > 0. \quad (2.5)$$

Finally, there is a further discrete constraint from K-theory which states that when we sum over all branes we must have [53]

$$\sum_a m_1 m_2 m_3 \equiv \sum_a m_1 n_2 n_3 \equiv \sum_a n_1 m_2 n_3 \equiv \sum_a n_1 n_2 m_3 \equiv 0 \pmod{2}. \quad (2.6)$$

To summarize, our problem is to find all sets of “ N_a -stacks” of supersymmetric branes, where N_a is a list of positive integers, for all values of the moduli (j, k, l) . A supersymmetric brane for moduli (j, k, l) is specified by a vector winding numbers $n_i^{(a)}, m_i^{(a)}$, which satisfy the SUSY conditions (2.4) or (2.1), as well as (2.5) and (2.6). An N_a -stack of branes is a set of supersymmetric branes taken with multiplicities N_a , which can be completed by adjoining zero or more additional distinct supersymmetric branes (with the same moduli) to give a configuration which satisfies Eq. (2.2). These additional branes will be called the “hidden sector” (note that they might or might not be physically observable in a particular model).

2.2 Types of branes

Our first step in solving this problem will be to classify the set of supersymmetric branes which are compatible with the positivity condition Eq. (2.5). This set has three components, distinguished by the number of nonzero tadpoles, which we will call the **A**-branes, **B**-branes and **C**-branes. They are as follows:

A) Four nonvanishing tadpoles:

In this case all n 's and m 's are nonzero. Let us categorize the allowed sign possibilities. First, note that changing the signs on any set of 4 winding numbers n_i, m_i, n_j, m_j amounts to an orientation-preserving coordinate redefinition and maps any configuration to one which is physically equivalent. Thus, we can without loss of generality choose signs so that either all n 's are positive or we have signs $+, +, -$. Let us first consider the case that all n 's are positive. If we choose all m 's positive then (2.4) and (2.5) cannot both be satisfied, since only $1/P$ in (2.4) is positive, and therefore $P < -Q/j$, for example, so the LHS of (2.5) would be negative. Changing signs on all m_i takes a brane to its image under Ω and leaves the tadpoles invariant, so we can assume that all branes contributing in the sum (2.3) with $n_1, n_2, n_3 > 0$ have signs for the m_i of $+ - -, - + -,$ or $- - +$. These three possibilities give tadpole combinations with 3 positive tadpoles and one negative, with Q, R, S respectively negative for the 3 choices of sign for the m 's. Now, assume the n 's have the signs $++-$. This gives a negative value for P , and to satisfy (2.4) we must have $Q, R, S > 0$, so without loss of generality we have signs $++-$ for the m 's.

To summarize, when all four tadpoles are nonvanishing, 3 must be positive and one negative.

B) Two nonvanishing tadpoles:

In this case just one of the n_i, m_i vanishes. This leads to two nonvanishing tadpoles and two vanishing tadpoles. A similar but simpler argument to that of case a)

shows that both nonzero tadpoles must be positive. Various choices of signs and which winding numbers vanish are possible, giving all 6 possible pairs of nonvanishing tadpoles.

C) One nonvanishing tadpole:

In this case at least two of the n_i, m_i vanish. But if precisely two vanish and there is one nonvanishing tadpole then there must also be precisely one nonvanishing term on the LHS of (2.1), which is impossible. So three winding numbers must vanish. In this case, however, primitivity implies that the nonvanishing winding numbers are all 1, so that the single nonvanishing tadpole is 1. Branes of this type do not contribute at all to (2.1) and thus do not constrain the Kähler moduli j_i . These are referred to as “filler” branes in some of the literature.

2.3 Symmetries

In this subsection we discuss the symmetries of the equations (2.4) and (2.5). We discussed above the symmetries of the n 's and m 's which map every brane configuration to a physically equivalent configuration. Changing signs on all m 's corresponds to switching branes under the action of the orientifold Ω . Changing signs on a pair of n 's and the same pair of m 's corresponds to an orientation-preserving coordinate change on the D-branes in the system. We use these symmetries to choose canonical forms for the values of n and m in brane configurations.

There is a further set of symmetries which acts on the set of solutions of (2.4), (2.5). This set of symmetries takes one solution to a distinct solution with different tadpoles. The obvious part of this set of symmetries arises from permutations on the 3 copies of T^2 , associated with the 6 permutations on the indices i . These symmetries also act on the tadpoles Q, R, S through the same permutation, and permute the moduli j, k, l in the same way.

This order 6 symmetry group can be extended further to include arbitrary permutations on all four tadpoles P, Q, R, S . The symmetry operation which exchanges P with one of the other four tadpoles corresponds to 90 degree rotations on two of the tori

$$\begin{aligned} n_i &\rightarrow m_i \rightarrow -n_i \\ n_j &\rightarrow m_j \rightarrow -n_j \quad . \end{aligned} \tag{2.7}$$

To extend this symmetry to the moduli j, k, l , we can write these moduli over a common denominator, $j \rightarrow j/h, k \rightarrow k/h, l \rightarrow l/h$, and then the permutation simply acts on the parameters h, j, k, l . When the original j, k, l are rational, we can replace the moduli with 4 integer parameters h, j, k, l .

This symmetry group corresponds to choices of coordinates on the original T^6 . We will find it useful to use this symmetry of the equations to simplify the discussion and analysis in several places in the remainder of the paper.

2.4 Proof of finiteness

In this subsection we prove that the number of models on the T^6/\mathbb{Z}_2^2 orientifold with a fixed number of brane stacks is finite. This implies among other things that the number

of models with any fixed gauge group is finite. In this subsection, and in the following subsections where we estimate the number of models with certain properties, we leave the total tadpole T as variable, though in the physical application for the given orbifold we have $T = 8$.

All the difficulty in proving finiteness arises from the **A**-type branes which can contribute negatively to Eq. (2.2). If we have only type **B** and **C** branes, it is immediately clear that there are a finite number of possible ways to saturate Eq. (2.2), since each brane stack with a winding number of absolute value N or more contributes at least N to some tadpole. Thus, we must have all winding numbers $\leq T$, which can be done in a finite number of ways, and we must have $\leq 4T$ brane stacks and images from that finite set of allowed brane stacks.

The analysis with the **A**-type branes must involve the supersymmetry conditions in an essential way, since one can find infinite sets of stacks by combining branes which are supersymmetric for different moduli [49].

We clearly cannot have an infinite family with only one **A**-type brane, since in an infinite family some winding number must be unbounded. This winding number contributes to two nonzero tadpoles, so with only one **A**-type brane it must contribute an unbounded positive amount to some tadpole which cannot be canceled by a negative contribution. This is a contradiction, so any infinite family must have more than one **A**-type brane. For the same reason, we cannot have an infinite family where only one tadpole takes unbounded values.

Now, let us consider the possibility of an infinite family where two tadpoles take unbounded values. Without loss of generality, let's assume these are the tadpoles R and S . Assume there are r **A**-type branes with tadpoles which are negative for R , and s **A**-type branes with negative S tadpoles. In the first case the tadpoles can be written $R = -a_i\nu_i, S = b_i\nu_i, i = 1, \dots, r$ where for each brane $\nu = |m_1|, a = n_2|m_3|$, and $b = n_3m_2$. In the second case the tadpoles can be similarly written $R = a'_i\mu_i, S = -b'_i\mu_i$. Because the other tadpoles are bounded, we have $0 \leq a_i, b_i, a'_i, b'_i \leq B$ for each i , where the upper bound is $B = T^2$ unless there are other branes with negative P or Q tadpoles. If there are an infinite family of configurations with a fixed number of branes and a fixed bound B , then there must also be an infinite number with some fixed combination of values for $a_i \dots b'_i$, so let us take these values as fixed. For these fixed values, the SUSY condition for the configuration with the smallest tadpoles tells us that there is a ratio $\lambda = l/k$ such that

$$b_i > \lambda a_i, \quad a'_i > b'_i/\lambda. \quad (2.8)$$

But now let us use this λ for the full infinite family and compute for each member of the family the sum

$$\sum (b_i - \lambda a_i)\nu_i + \sum \lambda(a'_i - b'_i/\lambda)\mu_i = T(\lambda + 1). \quad (2.9)$$

On the one hand, the RHS is fixed. But on the other hand, the LHS is a sum over linear terms in the ν_i, μ_i with fixed positive coefficients. So there cannot be solutions of this equation with arbitrarily large ν_i or μ_i and therefore there cannot be an infinite number of configurations where two tadpoles are unbounded and negative.

So we see that any infinite family of brane stack configurations solving the SUSY equations with a fixed number of stacks must have configurations with at least three \mathbf{A} -type branes and at least 3 of the tadpoles Q, R, S, T must be negative and unbounded on a sequence of \mathbf{A} -branes. We now proceed to prove that this situation also cannot occur.

Let us consider the sum over all \mathbf{A} -type branes

$$\sum_a P_a + \frac{1}{j} \sum_a Q_a + \frac{1}{k} \sum_a R_a + \frac{1}{l} \sum_a S_a \leq T \left(1 + \frac{1}{j} + \frac{1}{k} + \frac{1}{l}\right). \quad (2.10)$$

For each a , there is one negative tadpole, so the contribution for that a to the sum can be written using the equation (2.4) as, for example,

$$\left[P_a + \frac{Q_a}{j} + \frac{R_a}{k} - \frac{1}{\frac{1}{P_a} + \frac{j}{Q_a} + \frac{k}{R_a}} \right] + \dots \quad (2.11)$$

when $S_a < 0$ and similar expressions when one of the other tadpoles is negative.

But we can then use the elementary inequality

$$\frac{1}{x} + \frac{1}{y} + \frac{1}{z} > \frac{3}{x+y+z} \quad (2.12)$$

to show that

$$\sum_{a+} P_a + \frac{1}{j} \sum_{a+} Q_a + \frac{1}{k} \sum_{a+} R_a + \frac{1}{l} \sum_{a+} S_a \leq \frac{3}{2} T \left(1 + \frac{1}{j} + \frac{1}{k} + \frac{1}{l}\right), \quad (2.13)$$

where for each tadpole we only sum over positive contributions to that tadpole.

Now, using the symmetries discussed in the previous subsection, let us assume without loss of generality that $1 \leq j \leq k \leq l$. We then have an upper bound

$$\sum_{a+} P_a \leq 6T. \quad (2.14)$$

So we see that the sum of all positive P tadpoles is bounded above and therefore also that the negative tadpoles are bounded below by a limit proportional to the total tadpole number T .

We can now repeat this argument for Q . We have

$$\frac{1}{j} \sum_a Q_a + \frac{1}{k} \sum_a R_a + \frac{1}{l} \sum_a S_a \leq T \left(\frac{1}{j} + \frac{1}{k} + \frac{1}{l}\right). \quad (2.15)$$

Using the inequality

$$\frac{1}{x} + \frac{1}{y} > \frac{2}{x+y} \quad (2.16)$$

we then have

$$\frac{1}{j} \sum_{a+} Q_a + \frac{1}{k} \sum_{a+} R_a + \frac{1}{l} \sum_{a+} S_a \leq 2T \left(\frac{1}{j} + \frac{1}{k} + \frac{1}{l}\right), \quad (2.17)$$

so again

$$\sum_{a+} Q_a \leq 6T. \quad (2.18)$$

Thus, we see that two of the tadpoles are bounded in any infinite family, so there cannot be any infinite family where 3 tadpoles become unbounded. But the first part of the argument then shows that there cannot be any infinite families, since there cannot be any infinite families with only two unbounded tadpoles.

Combining these arguments, we see that any class of configuration with a definite number of stacks and thus a definite number of factors in the gauge group, contains finitely many configurations. To complete the argument that the total number of brane configurations is finite, we need to see that the number of factors in the gauge group is also bounded. This follows because the bounds we just obtained on the winding numbers do not depend on the number of stacks (beyond three). Thus the number of distinct supersymmetric branes is finite, and since each stack must contain a different supersymmetric brane, the number of possible stacks is finite.

2.5 Estimates

We can now use the analysis of the previous subsection to develop estimates for the numbers of brane configurations containing a particular gauge group and algorithms for enumerating these configurations.

First, because of the existence of the filler (type **C**) branes, any configuration which *undersaturates* each of the total tadpole constraints Eq. (2.2), can be completed to a configuration satisfying Eq. (2.2) by adding **C**-branes, in a unique way. Thus, the bulk of the problem amounts to enumerating N_a -stacks of **A**- and **B**-type branes satisfying

$$\sum_a P_a \leq T; \quad \sum_a Q_a \leq T; \quad \sum_a R_a \leq T; \quad \sum_a S_a \leq T. \quad (2.19)$$

In general, there are other configurations as well. First, part or all of the specified gauge group can be realized by **C**-type branes. These configurations are easy to get (of course one should keep in mind that adding further **C**-branes to saturate the tadpole will change the gauge group). Second, some configurations which violate Eq. (2.19) can be completed to satisfy Eq. (2.2), by adding hidden sector **A**-branes. We will neglect this possibility to start, and discuss **A**-type branes in the hidden sector later.

As we discussed earlier, there are straightforward bounds on the types and numbers of **B**- and **C**-type branes which can add up to a specified set of tadpoles. The difficulty is with the **A**-branes. One way to deal with them, which was taken in [40], is to scan over values of the moduli (j, k, l) . It follows immediately from (2.5) that the set of supersymmetric branes for any fixed moduli is finite. The problem with this approach is that one must then scan over all values of the moduli. Since the moduli need not be integers, this scan is far more difficult than the original problem. One might bring in number-theoretic arguments to bound the heights of the moduli, along the lines of [27], but this does not look easy.

A different approach, which we will follow here, is to find *a priori* bounds on the numbers and types of **A**-branes which can appear, which are independent of the moduli. We then enumerate all N_a -stacks, and then check for each whether all branes can simultaneously satisfy the condition Eq. (2.1) (note that we already found the general solutions to Eq. (2.5)). Since the equations Eq. (2.4) for **A**-branes are linear in the moduli (j, k, l) ,

as are Eq. (2.1) for **B**-branes, finding the moduli which solve them is an easy problem in linear algebra. We then keep only the configurations for which (j, k, l) are all positive.

This is a good approach if the fraction of all brane configurations (satisfying our *a priori* bounds) which turn out to be supersymmetric is not too small. For models with up to three stacks on T^6/\mathbb{Z}_2^2 , the equations Eq. (2.1) will always have solutions, of which a large fraction (more than $1/2^3$) turn out to be acceptable, so this approach works well.

On the other hand, if the number of brane stacks is greater than b_2 (the number of moduli, here 3), then the equations Eq. (2.1) are overdetermined, and this will be a problem. In this case, one could try a hybrid approach, in which one singles out a subset of b_2 brane stacks, enumerates all of these, and then completes each of these configurations by adjoining further brane stacks chosen to respect supersymmetry at the same (known) values of the moduli. However we will not need this approach here.

We now proceed by systematically analyzing the classes of models with one, two, and three stacks which undersaturate all tadpoles, discussing as we progress the effects of increasing numbers of **A**-type branes on the statistics. The upshot of this analysis is summarized in the last subsection of this section. Basically, we will find that when considering configurations of up to 3 brane stacks, a stack of N_b **B**-branes can be included in T^4/N_b^2 ways, while a stack of N_a **A**-branes can be included in T^3/N_a^3 ways. The reader not interested in the detailed arguments may wish to skip directly to subsection 2.6.

2.5.1 One-stack models

We begin our analysis by looking at how many different individual stacks of N branes undersaturate all tadpoles. As noted above, this does *not* tell us about all possible individual brane stacks which might appear as part of a model, due to the possibility of hidden **A**-type branes. This analysis, however, will get us going and indicate the nature of the problem we are considering. (Note that this does, however, give all possible individual brane stacks which can appear where all possible hidden-sector branes are type **B** or filler type **C** branes.) We begin by considering single branes (stacks with $N = 1$), and at the end of subsection describe the changes needed to incorporate larger values of N .

As discussed in 2.3 there are symmetries which permute the four tadpoles P, Q, R, S . Thus, we can simplify our analysis by putting the models we are interested in in canonical form. For a single brane this is particularly simple. We consider the three types of brane in turn

C: All possible type **C** branes are equivalent to the brane

$$\begin{aligned} (P, Q, R, S) &= (1, 0, 0, 0) \\ (n_1, n_2, n_3) &= (1, 1, 1) \quad (m_1, m_2, m_3) = (0, 0, 0). \end{aligned} \tag{2.20}$$

So up to symmetries there is a single type **C** brane.

B: All type **B** branes can be put in the form

$$\begin{aligned} (0, 0, R, S) &= (0, 0, pr, qs) \\ (n_1, n_2, n_3) &= (0, p, q) \quad (m_1, m_2, m_3) = (1, -r, -s). \end{aligned} \tag{2.21}$$

where $R \leq S$ and $p, q, r, s > 0$. (when $R = S$ we impose $p \leq q$.) The number of solutions of (2.21) in integers p, q, r, s with $R \leq S \leq T$ is approximately given by

$$\sum_{S \leq T} \sum_{R \leq S} d(R)d(S) \sim \frac{1}{2} T^2 (\ln T)^2 \quad (2.22)$$

where $d(N)$ is the number of divisors of N , and we have used $\sum_N d(N) \sim N \ln N$. The symmetry exchanging P and Q is given by (2.8) with $i, j = 2, 3$; this exchanges p with r and q with s along with some sign changes. Choosing a canonical form for each allowed brane reduces the number of distinct branes by another factor of 2. Thus, (2.22) gives a bound on the rate of growth of the number of individual type **B** branes which undersaturate all tadpoles

$$\mathcal{N}_b(T) \lesssim \frac{1}{4} T^2 (\ln T)^2. \quad (2.23)$$

Because of the primitivity condition, we must impose the further condition $(p, q) = (r, s) = 1$. This modifies the sum (2.22) to

$$\mathcal{N}_b(T) \sim \frac{1}{4} \sum_{r, s \leq T} \frac{T}{r} \frac{T}{s} \frac{\phi(r)}{r} \frac{\phi(s)}{s} \sim \frac{T^2 (\ln T)^2}{4\zeta(2)^2} = \frac{1}{4} \left(\frac{6}{\pi^2} \right)^2 T^2 (\ln T)^2 \quad (2.24)$$

where $\phi(n)$ is the Euler totient function giving the number of integers $< n$ which are relatively prime to n and $\zeta(s)$ is the zeta function $\zeta(s) = \sum n^{-s}$. A brief summary of the relevant features of the totient and zeta functions are given in Appendix A. The zeta function changes the overall constant to include the relative primality condition when summing over powers of various sets of integers, but does not change the scaling of the overall sum. In Figure 1 we plot the (log of the) upper bound (2.23) and the improved estimate (2.24) against the exact number of type **B** branes for general values of T . At $T = 8$ the bound gives 69.19, while the precise number of type **B** branes is $\mathcal{N}_b(8) = 71$, and the estimate (2.24) gives 42.06. Note that for small values of T the approximate bound (2.23) and the improved estimate (2.24) are exceeded because of configurations such as those with $R = S, p = q$, which are unchanged under some of the permutation symmetries. The estimate (2.24) is also poor for small T , since $\sum_{n < N} \phi(n)/n^2 \rightarrow \ln N/\zeta(2)$ converges to the asymptotic form slowly. Thus, we see that for type **B** branes the precise asymptotic form including number theoretic features is actually less reliable at the small physical value $T = 8$ than the rough estimate which ignores number theoretic subtleties. We continue to fix coefficients in this section including relative primality constraints, but in subsequent sections we will primarily concern ourselves with the main power law scaling of different kinds of branes.

A: Now, let us consider type **A** branes. These can always be put in the form $(-P, Q, R, S)$ for positive P and $0 < Q \leq R \leq S \leq T$. (As above, when tadpoles are equal we order on the corresponding n 's, and if these are equal we order on m to put the branes in canonical order; we choose all n, m positive except n_3, m_3 as in the discussion of Section 2.2.) The tadpole constraint puts an upper bound on the positive tadpoles Q, R, S . Given values of

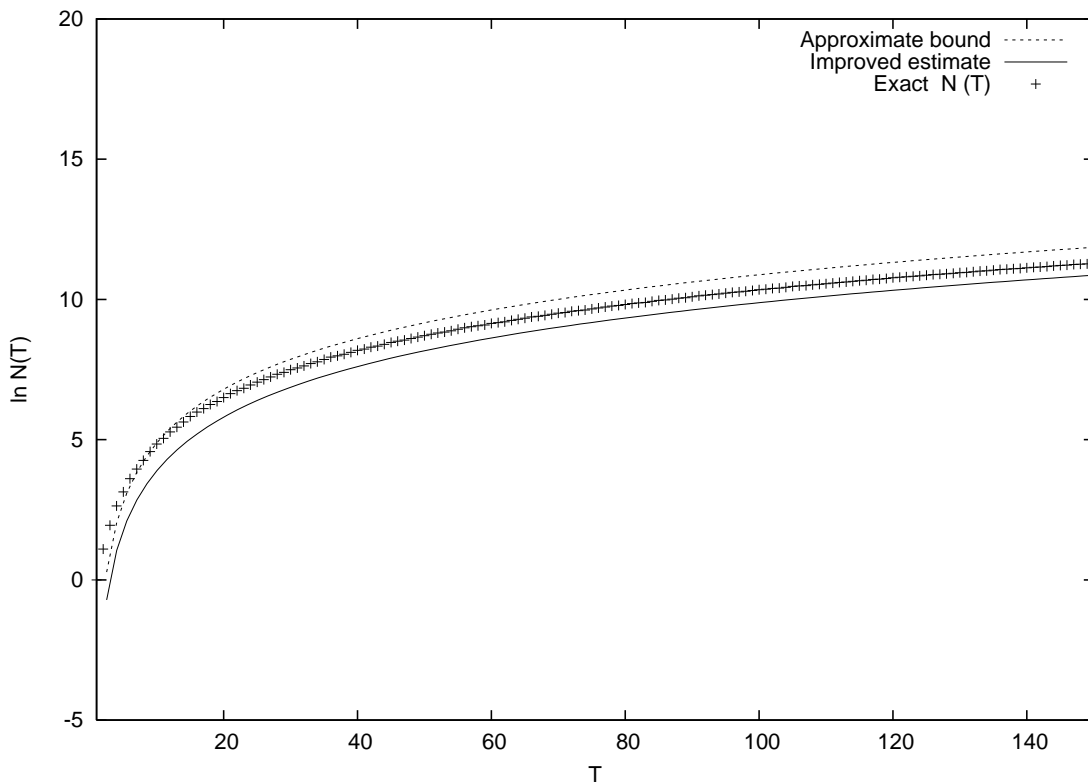


Figure 1: (Log of) number of type **B** branes for varying T

the m 's, we have the constraints

$$|n_i| \leq \frac{T}{\prod_{j \neq i} |m_j|} \quad (2.25)$$

This gives a simple upper bound on the number of type **A** branes which undersaturate all tadpoles

$$\mathcal{N}_a(T) \lesssim \frac{1}{6} \sum_{|m_i| \leq T} \frac{T^3}{\prod |m_i|^2} \lesssim \frac{1}{6} \left(\frac{\pi^2}{6}\right)^3 T^3 \quad (2.26)$$

Again, the actual number is smaller than the bound, even asymptotically, because of the primitivity conditions $(n_i, m_i) = 1$. The correction at large T to the upper bound (2.26) comes only from the relatively prime condition. This correction can be incorporated by replacing

$$\frac{\pi^2}{6} = \sum_n \frac{1}{n^2} \rightarrow \sum_n \frac{\phi(n)}{n^3} = \frac{\pi^2}{6\zeta(3)} \quad (2.27)$$

We graph the actual number of type **A** branes which satisfy the primitivity condition against the upper bound (2.26) and the estimate (2.27) in Figure 2. For $T = 8$, the bound gives 379.81, and the estimate gives 218.67, while the actual number of configurations is 226. In this case, because the sum $\sum 1/n^2$ converges quickly, the number theoretic corrections

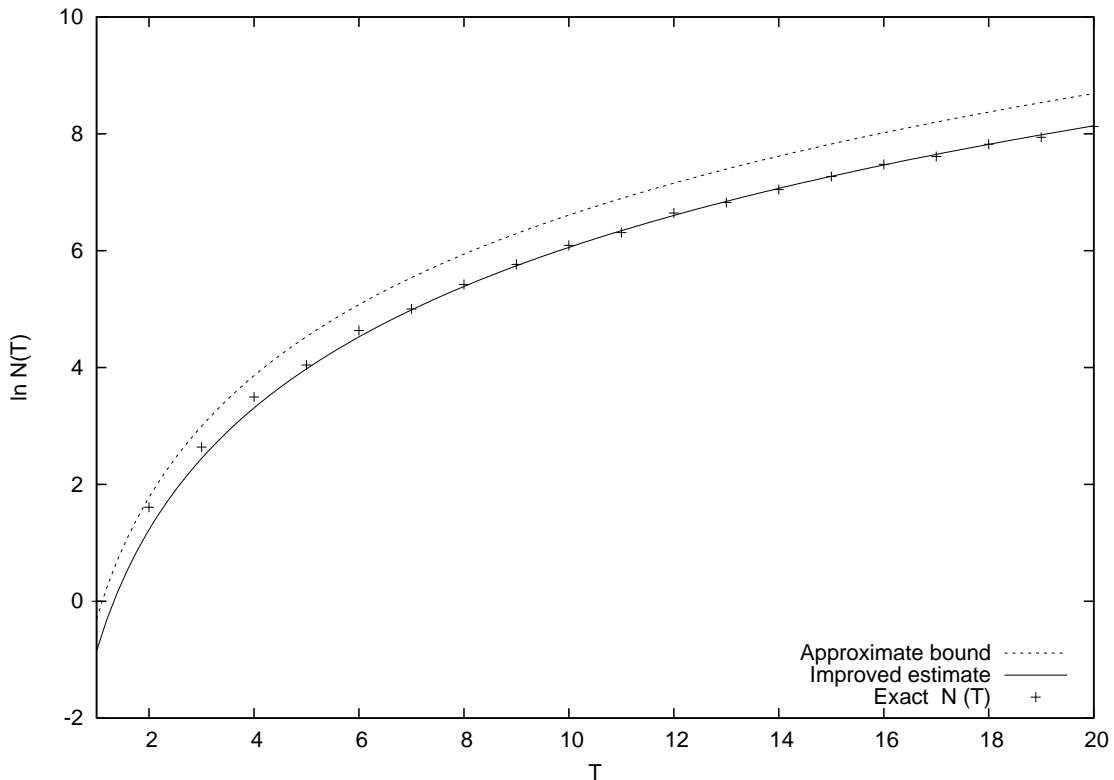


Figure 2: (Log of) number of type **A** branes for varying T

are correctly incorporated at a much smaller value of T so that the estimate including these corrections is very close. Again, the approximate bound and the estimate are exceeded for small T because of symmetric configurations (like $n, m = (1, k, k), (1, -1, -1)$); in this case, however, the bound rapidly exceeds the actual number even for small T because the sum in (2.26) is finite for finite T , and because for small finite T the number of allowed n_i is given by $\lfloor T/(m_j m_k) \rfloor$, which is generally smaller than $T/(m_j m_k)$.

We have now described in a systematic way how to estimate the number of single branes which undersaturate all the tadpole constraints, for each type of brane which can occur in this orientifold. To generalize the discussion to a stack of N branes, we simply take the formulae we have found above and replace $T \rightarrow T/N$, since the tadpoles from N copies of a given brane B are just N times the tadpoles of B .

Thus, we see that the number of stacks of N type **B** branes which undersaturate all tadpoles goes as

$$\mathcal{N}_{Nb} \sim \frac{9T^2(\ln T/N)^2}{\pi^4 N^2} \quad (2.28)$$

while the number of stacks of N type **A** branes which undersaturate all tadpoles goes as

$$\mathcal{N}_{Na} \sim \frac{\pi^6 T^3}{6^4 (\zeta(3))^3 N^3}. \quad (2.29)$$

Even for $N = 1, 2$, with $T = 8$ these numbers are quite small. For example, with $T = 8, N = 2$ we have $\mathcal{N}_{2a} = 33$, which is close to $1/2^3$ of the 226 found at $N = 1$, and reasonably close to the estimate (2.29), which gives 27.33, despite the small numbers involved. As discussed above, however, the presence of more type **A** branes introduces more negative tadpoles and makes it possible for many other individual branes to appear as part of combinations. The analysis in the case of multiple stacks can be carried out in a very similar way to the analysis of this subsection, though the details are more subtle. We describe multiple stacks in more detail in the following subsections.

2.5.2 Two brane stacks

We now consider the case of two distinct brane stacks. In this section we will just be concerned with determining the power in T with which different brane combinations scale, dropping constant and log factors. These factors could be included by a more careful analysis. As in 2.5.1, we begin by considering individual branes and then consider stacks of multiple branes.

AC, BC, CC: The case where one brane is type **C** is straightforward, as type **C** branes do not constrain the moduli and contribute to only a single tadpole. Up to symmetries, a pair of type **C** branes can appear in two ways, either contributing to the same tadpole or different tadpoles. Thus, the number of **CC** type branes is a constant

$$\mathcal{N}_{cc}(T) = 2. \quad (2.30)$$

Given a type **A** or type **B** brane, generically all symmetries are broken, and generically tadpoles are not saturated, so there are simply 4 ways to add a type **C** brane. So asymptotically the number of **AC** and **BC** combinations just go as 4 times the number of individual **A** and **B** branes. Dropping constants and log factors,

$$\mathcal{N}_{bc}(T) \sim \mathcal{O}(T^2) \quad (2.31)$$

and

$$\mathcal{N}_{ac}(T) \sim \mathcal{O}(T^3). \quad (2.32)$$

If we consider a stack of N type **C** branes and a stack of M type **B** branes, there is no constraint on the type **B** branes allowed if the stacks contribute to different tadpoles. So the number of $Mb + Nc$ combinations goes as (assuming $M, N \leq T$)

$$\mathcal{N}_{Mb+Nc}(T) \sim \mathcal{O}\left(\frac{T^2}{M^2}\right). \quad (2.33)$$

The situation is slightly more interesting for a combination of type **A** and type **C** branes. As we discussed above, a generic stack of M type **A** branes has tadpoles which scale as

$$M(-P, Q, R, S) \sim (-T^3/M^2, T, T, T), \quad (2.34)$$

so we can combine this with a stack of N type **C** branes for any $N \leq T^3/M^2$. Thus, there are order

$$\mathcal{N}_{Ma+Nc}(T) \sim \mathcal{O}\left(\frac{T^3}{M^3}\right) \quad (2.35)$$

combinations of M **A** branes and N **C** branes, with N allowed up to T^3/M^2 .

BB: A pair of **B**-type branes is straightforward. Two **B**-type branes can appear with the following four combinations of nonvanishing tadpoles, up to symmetries

$$(P, Q, 0, 0) + (P', Q', 0, 0) \tag{2.36}$$

$$(P, Q, 0, 0) + (P', 0, R', 0) \tag{2.37}$$

$$(P, Q, 0, 0) + (P', 0, 0, S') \tag{2.38}$$

$$(P, Q, 0, 0) + (0, 0, R', S'). \tag{2.39}$$

On the one hand, any combination of **B**-type branes which can appear individually can be combined in the form (2.39) so the number of **BB** combinations is at least as large as the square of (2.24). But on the other hand, with any of these combinations, each individual brane must be one we considered in the group estimated in (2.24), so the total number of **BB** combinations is bounded above by a small constant factor times (2.24) squared. Thus,

$$\mathcal{N}_{bb}(T) \sim \mathcal{O}(T^4). \tag{2.40}$$

It is actually straightforward to show that, more precisely, $\mathcal{N}_{bb}(T) \sim 3/(4\zeta(2)^4)T^4(\ln T)^4$.

Following the same analysis, the number of ways in which a pair of stacks of N, M **B** type branes can be combined goes as

$$\mathcal{N}_{Mb+Nb}(T) \sim \mathcal{O}\left(\frac{T^2}{M^2} \cdot \frac{T^2}{N^2}\right), \tag{2.41}$$

where the two factors represent the ways in which the M and N stacks can be individually realized.

AB: Now we consider combining an **A** brane with a **B** brane. Here the story becomes more interesting. As in our discussion of **AC** combinations, because the **A** brane can have tadpoles which scale as

$$(-P, Q, S, R) \sim (-T^3, T, T, T) \tag{2.42}$$

we can include type **B** branes with tadpoles of order

$$(P', Q', 0, 0) \sim (T^3, T) \tag{2.43}$$

(and similar **B** branes with nonvanishing tadpoles P', R' and P', S') The analysis of the number of **B** branes with tadpoles of this order proceeds just as in the discussion leading to (2.23), but now the number of possible branes goes as $T^4(\ln T)^2$. It is straightforward to check that for any such **AB** combination there is a set of moduli j, k, l which satisfy the SUSY equations (2.1) for both branes. The **B** brane in (2.43) has $m_1 = 0$, so the tadpole condition (2.1) just constrains the ratio of moduli k/l . Putting the tadpoles from the **A** brane into (2.4) we see that k, l can always be taken to be sufficiently small that there is a solution for j , for any ratio k/l . A similar argument holds for the other sets of order T^4 **B** branes. Thus, the number of **AB** combinations goes as (dropping the logs)

$$\mathcal{N}_{ab}(T) \sim \mathcal{O}(T^7). \tag{2.44}$$

Note that there are also order T^5 configurations where the **B** brane contributes to two of the tadpoles Q, S, R , but these are subleading and we will drop them.

The number of ways in which stacks of M type **A** branes and N type **B** branes can be combined can similarly be computed to be

$$\mathcal{N}_{Ma+Nb}(T) \sim \mathcal{O}\left(\frac{T^7}{N^2 M^5}\right), \quad (2.45)$$

where the extra factor of $1/M^2$ appears as an extra suppression factor on the number of **B** branes because of the P tadpole in (2.34).

At this point we see explicitly the phenomenon mentioned above, that inclusion of additional type **A** branes can increase the number of ways a given combination of stacks can be realized. While the number of individual type **B** branes which undersaturate all tadpoles goes as T^2 , in the presence of a stack of type **A** branes, there are T^4 type **B** branes which may appear. A more complete discussion of this effect is given in subsection 2.5.4.

AA: We now consider the case of two (stacks of) **A**-type branes. This case is more complicated because each brane can have a different negative tadpole. (The number of combinations where both branes have the same negative tadpole just goes as $\mathcal{N}_a^2 \approx T^6$.) We can, up to symmetries, choose the two branes to have tadpoles¹

$$(-P, Q, R, S) = (-a\nu, b\nu, m_1 n_2 m_3, m_1 m_2 n_3) \quad (2.46)$$

$$(P', -Q', R', S') = (a'\nu', -b'\nu', m'_1 n'_2 m'_3, m'_1 m'_2 n'_3) \quad (2.47)$$

where $a = n_2 n_3, b = m_2 m_3, \nu = n_1$ and similarly for the primed variables. This now fits directly into the context of the proof of finiteness for configurations with two negative tadpoles in (2.4). From the SUSY condition we must have

$$\frac{b}{a} > \frac{b'}{a'} \quad (2.48)$$

Because of the bound (2.9), we must have

$$(b - \lambda a)\nu + \lambda(a' - b'/\lambda)\nu' \leq T(\lambda + 1) \quad (2.49)$$

for any λ such that $b/a > \lambda > b'/a'$. Since $a, b, a', b' \leq T$, this bounds the number of possible values of ν, ν' which can satisfy (2.49).

Let us now compute the number of possible values of ν' and ν compatible with the SUSY conditions for a fixed set of values a, b, a', b' . The two individual tadpole conditions are

$$b\nu - b'\nu' \leq T, \quad a'\nu' - a\nu \leq T. \quad (2.50)$$

Because $a'/a > b'/b$, along with $\nu', \nu > 0$ these inequalities define a convex quadrilateral region in the ν', ν plane whose boundary has vertices

$$\begin{aligned} (0, 0) & \qquad (T/a', 0) \\ (0, T/b) & \qquad \left(\frac{a+b}{a'b-ab'}T, \frac{a'+b'}{a'b-ab'}T \right). \end{aligned} \quad (2.51)$$

¹In this argument only, we are using different sign conventions $m_i, n_i > 0$ from elsewhere in the paper.

We can use this quadrilateral both to estimate the number of allowed **AA** brane combinations, and to determine the largest tadpoles allowed for P, Q' .

Now, let us consider the ways in which a, b, a', b' can be chosen. Choosing $m_1 > 1$ essentially reduces $T \rightarrow T/m_1$ in the selection of a, b, \dots which leads to suppression by a factor of m_1^2 , so the most general configurations will have $m_1 = m'_1 = 1$, with other values of m_1, m'_1 just giving rise to an overall constant factor of $\zeta(2)^2$. We will not be extremely careful about constant terms but will just keep around the obvious ones to get a heuristic picture of the overall constant coefficient. Next, we can sum over all $n_2, n_3 \leq T$ and then all $m_2 \leq T/n_3$ and $m_3 \leq T/n_2$, and similarly for the primed variables. This will lead to on the order of $T^4(\ln T)^4$ possibilities. The constraint (2.48) gives another constant factor of $1/2$.

At this point let us consider three cases:

- i) $b/a > b'/a' > 1$
- ii) $b/a > 1 > b'/a'$
- iii) $1 > b/a > b'/a'$

In each of these cases, $a'b > ab'$. Let us first assume that the difference is of the same order as the larger term, $a'b - ab' \sim a'b$, so that we can drop the smaller term in computations. In this approximation, we find the following leading terms for the tadpoles of the two branes in the three cases:

i) Here

$$P = a\nu \sim \frac{ab'}{a'b}T < T, \quad Q = b\nu \sim \frac{b'}{a'} \leq T^2 \quad (2.52)$$

where we have used $b'a' \leq T^2$. Similarly for P', Q' , so the largest tadpoles possible in this case are

$$\begin{aligned} (-P, Q, R, S) &\sim (-T, T^3, T, T) \\ (P', -Q', R', S') &\sim (T, -T^3, T, T). \end{aligned} \quad (2.53)$$

ii) A similar analysis shows that the largest tadpoles possible here are

$$\begin{aligned} (-P, Q, R, S) &\sim (-T, T, T, T) \\ (P', -Q', R', S') &\sim (T, -T, T, T). \end{aligned} \quad (2.54)$$

iii) In this case the largest tadpoles possible are

$$\begin{aligned} (-P, Q, R, S) &\sim (-T^3, T, T, T) \\ (P', -Q', R', S') &\sim (T^3, -T, T, T). \end{aligned} \quad (2.55)$$

In this analysis we have assumed that $a'b - ab' \sim a'b$, dropping the second term. The exact area of the quadrilateral (2.51) is

$$\frac{1}{a'b - ab'} \left(1 + \frac{a}{2b} + \frac{b'}{2a'}\right) T^2. \quad (2.56)$$

This is a measure of the number of ν, ν' 's which are allowed for fixed a, b, a', b' . We see that in case *ii* the term in parentheses is dominated by 1, and since generically $aa'bb' \sim T^2$ and $a'b > ab'$ the area generically in this case is order 1 or less. In cases *i* and *iii* we have a term in parentheses which can be as large as T^2 . Thus, we expect of order T^2 possible ν, ν' 's in these cases. These numbers of ν, ν' 's correspond to the numbers of ways we can choose the extra factors for the P, Q tadpoles in (2.53-2.55). From this analysis we expect cases *i* and *iii* to dominate, with another constant factor of $1/2$ to select these cases.

Finally, however, we must look at the denominator term $a'b - ab'$ in (2.56). Generically we expect that this number will be distributed fairly uniformly amongst numbers of order T^2 . For roughly $1/T^2$ of configurations this denominator will take the value 1. For these special configurations, the range of possible values for ν, ν' each get an extra factor of T^2 . For these configurations, we can read off the maximum values for the tadpoles, which become in case *iii*

$$\begin{aligned} (-P, Q, R, S) &\sim (-T^5, T^3, T, T) \\ (P', -Q', R', S') &\sim (T^5, -T^3, T, T). \end{aligned} \tag{2.57}$$

Note, however, that the maximum values of these tadpoles, and the largest value of (2.56) will only arise when $a, a' \sim T^2, b, b' \sim 1$. In this case $m_2, m_3, m'_2, m'_3 \sim 1$ and the log factors are dropped when computing the number of possible a, a' 's, but we probably get another log from the b' in the denominator of the $a'/2b'$ in parentheses in (2.56). We thus expect that the number of configurations of this type will go as the number of a, a', b, b' 's ($\sim T^4$), multiplied by the frequency with which $a'b - ab' = 1$ ($\sim 1/T^2$), multiplied by the number of possible ν, ν' 's (T^4) for an overall result of $T^6(\ln T)^4$. When $a'b - ab' = 2$, we have a similar phenomenon but now the area (2.56) gets an additional factor of $1/2$. Summing over all values, we expect an additional log. A similar number of configurations should be possible in case *i*, while the number of configurations of case *ii* is suppressed by T^2 .

Summing up the discussion, we expect that the number of **AA** brane combinations should go (up to some slop in the overall constant, and perhaps also in the power of the log) as

$$\mathcal{N}_{aa}(T) \sim \mathcal{O}(T^6). \tag{2.58}$$

A rough estimate of the constant coefficient and powers of logs suggests that this should go more precisely as something like $\zeta(2)^2(\ln T)^2/32$. These factors should not be taken too seriously except to note that the overall constant is small; combined with the logs this gives a factor of roughly 0.16 at $T = 4$.

Incorporating the dependence on stack sizes is slightly more subtle in this case. In the total number of combinations of N **A**-stacks of one kind and M **A**-stacks of another kind, there may be several terms in which have different scalings. We should have an overall suppression by at least N^2M^2 since ab is suppressed by N^2 and $a'b'$ is suppressed by M^2 . Furthermore, the overall power of N, M in the denominator must match the power of T in the numerator, so we have schematically

$$\mathcal{N}_{Ma+Na}(T) \sim \mathcal{O}\left(\frac{T^6}{N^2M^2}P_2(1/N, 1/M)\right) \tag{2.59}$$

where $P_2(1/N, 1/M)$ is a homogeneous polynomial of degree 2 in its arguments.

In the case we have considered here the values of one negative tadpole can be as low as $-\mathcal{O}(T^5)$, when the scaling of the tadpoles goes as in (2.57). We have checked this result numerically and found agreement; note however that the coefficient in front of the T^5 is something like $1/32$, since the largest possible value of $a \sim a'$ goes as $T^2/4$. For $T = 8$, the most negative tadpole allowed is $P = -792$.

It is also of interest to consider how large the total tadpole from the two **AA** branes can be. We note first that only one total tadpole (at most) can be negative. Indeed, if both were negative we would need to have $a > a', b' > b$ which contradicts $b/a > b'/a'$. Now let us ask how negative that negative tadpole can be. Assume we are in case *iii*, so $a > b, a' > b'$. Then we want a lower bound on the (possibly negative) total tadpole $a'\nu' - a\nu$. From (2.50) we see that

$$\nu \leq \frac{T + b'\nu'}{b} \Rightarrow a\nu \leq T\frac{a}{b} + a'\nu' \quad (2.60)$$

from which it follows

$$a'\nu' - a\nu \geq -T\frac{a}{b} \geq -T^3. \quad (2.61)$$

Thus, while the individual tadpoles can scale as (2.57), the sum of the two tadpoles must scale as

$$(P' - P, Q - Q', R + R', S + S') \sim (-T^3, T, T, T) \quad (2.62)$$

or just the same as a single **A**-type brane. We will find this result useful in our further analysis of more complicated configurations.

To summarize the results of our analysis, in this subsection we have shown that the numbers of **BB**, **AB**, and **AA** combinations of brane stacks which admit some common Kähler moduli and which undersaturate all the tadpole conditions go as T^4, T^7, T^6 respectively. We have explicitly computed the number of such combinations up to $T = 8$ (for stacks containing a single brane). The results of this explicit computation are shown in Figure 3. Note that we have connected the data points with lines for clarity, but we have not graphed the explicit analytic predictions, which like the case of **B** branes (2.24) converge slowly due to the log factors. As predicted, the number of **AB** branes is the largest, and the number of **AA** branes grows faster than the number of **BB** branes, but the **AA** and **BB** curves cross since the **AA** coefficient is much smaller than the **BB** coefficient.

At $T = 8$ we find that the exact numbers of brane combinations are

$$\mathcal{N}_{aa}(8) = 30,255 \quad (2.63)$$

$$\mathcal{N}_{ab}(8) = 434,775 \quad (2.64)$$

$$\mathcal{N}_{bb}(8) = 20,244 \quad (2.65)$$

The numbers at $T = 4$ are

$$\mathcal{N}_{aa}(4) = 264 \quad (2.66)$$

$$\mathcal{N}_{ab}(4) = 3,029 \quad (2.67)$$

$$\mathcal{N}_{bb}(4) = 558 \quad (2.68)$$

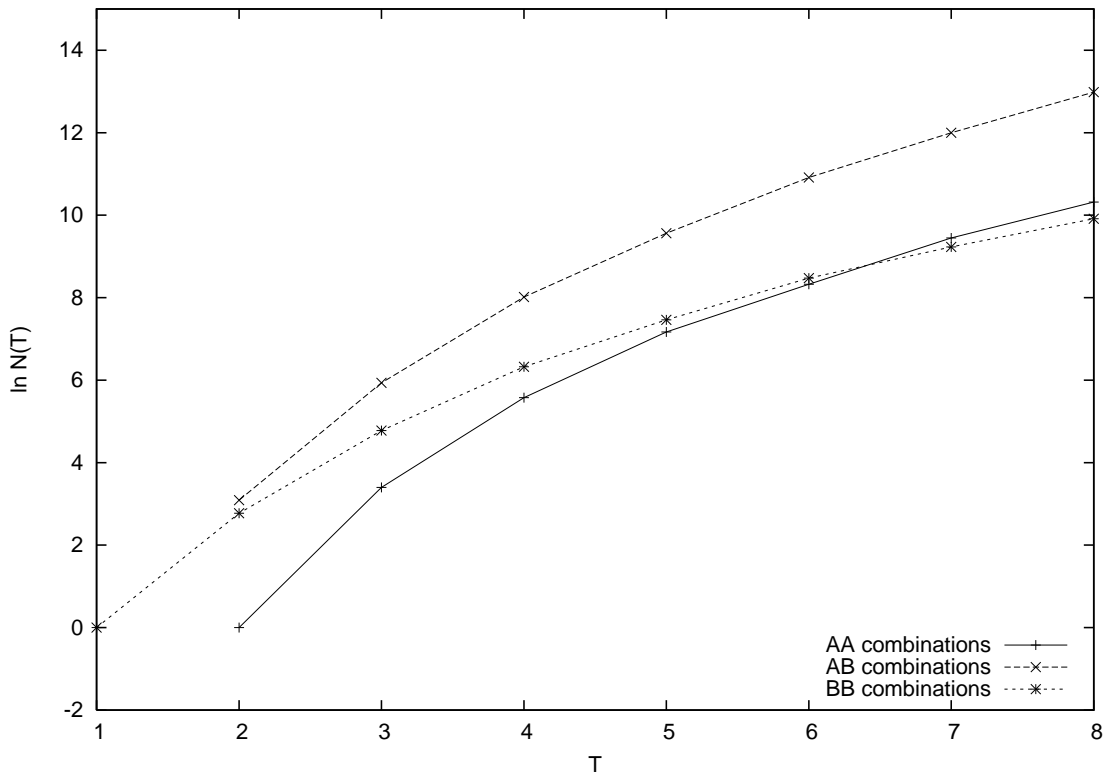


Figure 3: (Log of) number of type **AA**, **AB**, **BB** branes for varying T

These configurations are equivalent to brane stacks with all $N = 2$ at $T = 8$, and are suppressed relative to the $N = 1, T = 8$ results above by approximately the expected factors of $2^6, 2^7, 2^4$, though in each case growth is slightly faster due to logs.

2.5.3 Three stacks

From the complications in the preceding argument for the number of two-stack **AA** configurations, one might worry that the problem will become increasingly more complicated, and tadpoles will become increasingly more negative as more type **A** branes are included. Fortunately, however, from the second part of the finiteness argument, we know that two tadpoles can have maximum total positive contribution of $6T$. Thus, branes with the other two tadpoles negative are constrained by the same type of argument as in the above **AA** analysis, with the only difference being that the a, b, \dots are constrained by a factor of $6T$ instead of T . Thus, no matter how many branes we have, the largest tadpoles can have absolute value no larger than T^5 and the second largest no larger than T^3 as in (2.57). Furthermore, when pairs of **A**-type branes are considered their total tadpoles must scale as (2.62), or just as a single **A**-type brane. This simplifies the analysis of configurations with more branes.

In this subsection we briefly describe three-stack configurations of various types. We content ourselves with some simple scaling arguments and polynomial bounds on the rate

of growth of various combinations.

Let us begin with **BBB** combinations. It is straightforward to see that by choosing 3 different pairs of tadpoles for the three **B**-type branes we have order T^6 configurations. For N, M, L **B**-type stacks, the number of possible configurations goes as

$$\mathcal{N}_{Nb+Mb+Lb}(T) \sim \mathcal{O}\left(\frac{T^6}{N^2M^2L^2}\right). \quad (2.69)$$

Now consider **BBA**. If we take an **A**-type brane with tadpoles of order $(P, Q, R, S) \sim (-T^3, T, T, T)$, then we can consider **B**-type branes with P, Q and P, R tadpoles. There are T^4 of each type of **B** brane possible. These branes fix the ratios of moduli $k/l, j/l$ and are compatible with any **A** type brane with negative P tadpole by just taking all of j, k, l small enough. Thus, there are T^{11} possible combinations of this type. For N, M -stacks of **B** branes and an L stack of **A**-branes, we have

$$\mathcal{N}_{Nb+Mb+La}(T) \sim \mathcal{O}\left(\frac{T^{11}}{N^2M^2L^7}\right) \quad (2.70)$$

where as in the **BA** case, the numbers of each kind of **B** brane are suppressed by an extra factor of L^2 .

Now consider **BAA**. Since any **AA** combination has tadpoles which scale at worst as (2.62), or just as a single **A**-type brane, we again can have at most order $\mathcal{O}(T^4)$ choices for the type **B** brane. Let us assume that the **b** brane has nonzero tadpoles P, Q . Such a brane puts a constraint on the ratio of moduli k/l , but this constraint can be made compatible with any two mutually compatible **a** branes with negative tadpoles in P, Q by just making k, l small enough. Thus, the number of **BAA** branes should go as T^{10} . For a N -stack of **B** branes and M, L **A** stacks, we have

$$\mathcal{N}_{Nb+Ma+La}(T) \sim \mathcal{O}\left(\frac{T^{10}}{N^2M^2L^2}P_2(1/M, 1/L)\right). \quad (2.71)$$

Finally, consider **AAA**. Since as shown in (2.62), any two of the **A**-type branes must have a total tadpole of the same form as a single **A**-type brane, combining with a third **A**-type brane seems to lead to at most an additional factor of T^3 . Since not all sets of 3 **A**-type branes are mutually compatible with any common set of moduli, this leads to an expected upper bound on the number of **AAA** combinations

$$\mathcal{N}_{Na+Ma+La}(T) \sim \mathcal{O}\left(\frac{T^9}{N^2M^2L^2}P_3(1/N, 1/M, 1/L)\right). \quad (2.72)$$

Because this family of configurations is subleading, and we will not use it in any specific model-building constructions, we do not carry the analysis of 3 **A**-stack configurations further here. It should be possible, however, to analyze this set of configurations in more detail using the constraints from the proof of finiteness and methods like those used in the two **A**-stack analysis of the previous subsection. We leave a further analysis of this type for future work.

2.5.4 Hidden sector **A**-type branes

We have found that including **A**-type branes can enhance the number of ways of including brane stacks, particularly of **B**-type branes. One might worry that with more and more **A**-type branes in the hidden sector, more and more brane combinations could be realized in the visible sector for a given gauge group. This does not happen, however, essentially because of (2.62). To see this concretely, let us return to the number of ways we can include a $U(N)$ factor in our gauge group from N type **B** branes. In the absence of **A**-type branes, the number of possible stacks (2.24) went as T^2/N^2 (dropping logs). As we found in (2.43), the inclusion of an **A**-type brane in the hidden sector increases this to order T^4/N^2 . From (2.62), however, we see that even when two **A** branes are included in the hidden sector the number of possible **B**-type branes still goes as T^4/N^2 . In fact, when a second **A**-type brane is added in the hidden sector, no new type **B** branes at all become possible, since the limits on the tadpoles of the type **B** brane are the same as with a single **A** brane in the hidden sector, and, as we showed in the discussion above, all **B** branes with a nonzero tadpole where the single **A** brane has a negative tadpole and which undersaturate the total tadpole condition can be realized for some values of the moduli. Thus, we see that no matter how many **A**-type branes are included in the hidden sector, including a stack of **B**-type branes will always give rise to a factor of order T^4 in the total number of possible models.

How about type **A** branes where a type **A** brane is included in the hidden sector? From the analysis of **AA** combinations in 2.5.2 we note that in the order T^6 cases where $a'b - ab' = 1$ and $b = b' = 1, a \sim \mathcal{O}(T^2)$, the first brane can be chosen in (T^5) different ways. The second brane is then constrained to have $a' = a + 1$, and ν' has a range of size T from the quadrilateral (2.51). So for each of the order T^5 choices for the first brane there are order T choices for the second brane. This shows that with a hidden **A**-type brane, there can be T^5 **A**-type branes in the visible sector. As for the **B** branes, however, the presence of another **A**-type brane in the hidden sector cannot increase the number of possible branes in the visible sector, since the additional hidden brane cannot change the scaling of the tadpoles. By a similar argument to that above for type **B** branes, we expect that even with an arbitrary number of **A**-type branes in the hidden sector, the scaling of the number of models will get a factor of at most T^5 from the first **A**-stack, and at most T^3 from subsequent stacks, though we do not have a complete proof of this assertion.

2.6 Summary of results

In summary, we have found that we can give an approximate asymptotic upper bound for the number of models with any desired gauge group appearing as a subgroup by including a polynomial factor of

$$\hat{\mathcal{N}}_{N_b b} = \frac{T^4}{N_b^2} \quad (2.73)$$

for each stack of N_b **B**-type branes. This factor does not include some additional log factors which may be particularly relevant at small T and assumes that there is at least one **A** brane in the hidden sector; if there are no **A** branes in the hidden sector the factor is

reduced to T^2/N_b^2 . Assuming a hidden sector **A** brane, a factor of

$$\hat{\mathcal{N}}_{N_a a} = \frac{T^5}{N_a^2} \quad (2.74)$$

must be included for the first stack of N_a **A**-type branes; this factor reduces to T^3/N_a^3 in the absence of hidden sector **A** branes. We are fairly sure, though we have not definitively proven, that the contribution to the upper bound from the second and further stacks of **A**-type branes can be reduced to

$$\hat{\mathcal{N}}_{N_a a} = \frac{T^3}{N_a^2} \quad (2.75)$$

whether or not there are hidden sector **A**-type branes. For gauge groups with many factors, the product of these expressions will give an upper bound, but the actual number will be fewer as the moduli will be overconstrained. As an example, the number of ways in which the Pati-Salam gauge group $U(4) \times U(2) \times U(2)$ arises from **AAB** combinations (assuming a hidden sector **A** brane) is bounded from the above estimates as $T^{12}/2^8 \sim 3 \times 10^8$. In practice, we expect that this is an overestimate and that the largest number of combinations may come from **ABB** combinations. We will discuss explicit model building further in Section 4.

We emphasize again that the configurations we are counting are those in which a desired gauge group is realized as part of a complete model which saturates the tadpoles. For any given gauge group which we impose as a subgroup of the full UV gauge group arising from the intersecting branes, each of the polynomial number of configurations we are counting will have a large number of possible completions to a complete model. Generally the number of “hidden sector” completions will go roughly as e^{T-T_m} where T_m characterizes the tadpole contribution from a given model which undersaturates the complete tadpole cancellation condition. By analyzing the different ways in which the desired group can be realized as a piece of an intersecting brane model, we reduce the problem of analyzing the space of models to a polynomial problem. We can analyze this polynomial number of solutions for configurations of physical interest, and then in principle we could go on to do a systematic analysis of the hidden sector possibilities in models of particular interest.

2.7 Algorithms

In this section we have focused first on proving that the number of models which contain a desired gauge group is finite, and then on using the insight from the proof of finiteness to estimate the number of models with a given gauge group. We can also, however, use the same methods used to give estimates for the number of models with particular brane types and stack sizes to construct algorithms which explicitly enumerate these models. In general, these algorithms can be extremely efficient, and have time and memory requirements roughly in proportion to the number of solutions being constructed.

To be more explicit, consider the problem of explicitly enumerating one of the classes of branes we have described above. Assume first that we have already constructed some brane configuration with total tadpoles $P, Q, R, S \leq T$, and we wish to construct all possible ways of including a stack of N type **B** branes while still undersaturating all tadpoles. As in the

discussion proceeding (2.22), we are searching for sets of four integers satisfying constraints like $pr \leq T - R, qs \leq T - S$. By simply looping over $p \leq T - R$ and then looping over $r \leq \lfloor (T - R)/p \rfloor$, we can search for all allowed pairs p, r in time $(T - R) \ln(T - R)$, which is roughly the number of solutions expected, and similarly for q, s . This gives us a candidate set of allowed type **B** branes to include, and we can then explicitly check the SUSY conditions for each possibility. This procedure can be iterated to include an arbitrary number of **B**-type stacks, and **C** type stacks can be included by simply checking which tadpoles are not saturated.

This leaves us with the problem of constructing algorithms for finding combinations of stacks of type **A** branes. Using the bounds on individual tadpoles from these branes which we found in the proof of finiteness, we can readily construct such algorithms. For single **A** branes with for example a negative P tadpole, we just loop over all possible values of the n 's and m 's which have $Q, R, S \leq T$. As in (2.25), this can be done in time of order T^3 and generates $\mathcal{O}(T^3)$ possible **A**-type branes.

A pair of **A**-type branes with the same negative tadpole can be constructed by just repeating the single **A** brane procedure, constraining the sum of the positive tadpoles. For a pair of **A**-brane stacks with different negative tadpoles, we proceed as in the **AA** analysis in subsection 2.5.2. We first loop over possible values of n_2, n_3, m_2, m_3 and similar for the primed variables. This gives a, b, a', b' , which define the quadrilateral (2.51), which we can then scan over for all possible values of ν, ν' . This generates a set of candidate **AA** possibilities which we can then check for the existence of moduli satisfying the SUSY constraints.

Constructing a set of three **A**-type branes proceeds again in a similar fashion. The worst case here is when all three type **A** branes have different negative tadpoles. Because of the bounds (2.14, 2.18), however, we know that the sum of positive tadpoles is bounded by $6T$ for one of the tadpoles which has a negative contribution from one **A**-brane. (In fact, a more careful analysis shows that in this 3-brane case the sum is bounded by $2T$, which helps with constant factors but not with scaling.) From this, we can sum for the first two **A**-branes as in the above **AA** discussion, just keeping (without loss of generality) $S_1 + S_2 \leq T, R_1 + R_2 \leq 2T$. We construct all possible pairs under these conditions which undersaturate the tadpoles P, Q as above. We can then enumerate all possible third **A**-branes given the resulting upper bounds on all tadpoles besides R .

For more than three **A**-type branes, we can generalize this analysis. Basically the idea is that the tadpole constraints combined with inequalities like (2.48) coming from the SUSY constraints lead to a set of inequalities like those determining the quadrilateral (2.51), so that we can loop over the various winding numbers and construct a set of allowed combinations of k distinct **A**-brane stacks in time of order T^{3k} . For $k > 3$, however, the SUSY conditions generically will overdetermine the moduli, so this approach becomes less and less efficient as the fraction of SUSY-allowed combinations decreases. To construct all configurations with larger numbers of type **A** branes, it is probably most efficient to first construct all combinations which are large enough to uniquely determine the moduli (which will generically be 3 **A** brane stacks but may be more in special cases). Then, one can construct all **A**-type branes which are compatible with a particular set of moduli. The

number C_m of such branes must be finite for any set of moduli m because of the inequality (2.5) which imposes a positive-definiteness condition on the tadpoles for fixed values of the moduli. If the number of stacks required to fix the moduli was d , we can then check all C_m^{k-d} possible ways of combining these branes into a configuration which undersaturates all tadpoles. This gives a complete algorithm for constructing all allowed configurations of k type **A** brane stacks.

3. Distribution of intersection numbers

Now that we have a systematic approach to estimating the number of brane configurations realizing a desired gauge group, and efficient algorithms for generating such configurations, we want to analyze some further physical features of these different models. The simplest next feature to analyze is the intersection number between branes, which determines the number of chiral fermions associated with strings connecting these branes [6]. These chiral fermions transform in the fundamental representation of the gauge group associated with one brane and in the antifundamental representation of the gauge group associated with the other brane. We will not discuss the non-chiral spectrum other than to recall that all of the branes we are using (on the torus orientifold) have adjoint matter, and that other vector-like matter (such as the Higgs doublets) is obtained by taking pairs of branes which coincide along one axis (*i.e.* with the same (n_i, m_i) for some i).

In this section we will look at the distributions of intersection numbers for combinations of different types of branes. There are several motivations for considering these distributions. Most generally, we are interested in looking for correlations of any kind in the landscape of string vacua. As discussed in the introduction, such correlations are ultimately necessary to make predictions, assuming that all string vacua are viable. A strong correlation, such as an observation that all string models of this type with 3 generations of quarks also have 3 generations of leptons, would be very suggestive and would motivate looking for similar correlations in other regions of the landscape. On the other hand, a smooth broad distribution of intersection numbers with no correlations suggests that it may be difficult to use string theory to predict the number of generations found in nature. As a more specific application, we can use the distributions of intersection numbers to estimate what fraction of the total set of models with a fixed gauge group have a given number of generations (like 3). We carry out such an estimate in the next section using the results developed in this section.

To understand the correlations between different intersection numbers, it is useful to introduce the information theory notion of *mutual entropy*. Given a probability distribution on possible values of a variable x , where p_i is the probability that $x = i$, the (base 2) *entropy* of x is defined to be

$$H(x) = - \sum_i p_i \log_2 p_i. \quad (3.1)$$

This quantity expresses the number of bits of information which are needed on average to encode a given instance of the random variable x . (For example, if $x = 1, 2$ each have probability 1/4, and $x = 3$ has probability 1/2, then $H(x) = 3/2$; if $x = 3$ we can encode

this in the bit 0, and we can encode $x = 1, 2$ in the two-bit sequences 10, 11.) Given a distribution on two variables x, y , the mutual entropy is defined to be

$$\mathcal{I}(x, y) = H(x) + H(y) - H(x, y). \quad (3.2)$$

The mutual entropy, also called the relative entropy, encodes the number of bits of information given about y if x is known (or vice versa). If two variables are completely independently distributed, then $\mathcal{I} = 0$ (knowing x gives no information about y). If two variables are completely correlated, so that there is a one-to-one function relating values of x with associated values of y then $\mathcal{I}(x, y) = H(x) = H(y)$.

Now, let us define the winding numbers whose distributions we are interested in. If we have two brane stacks, where the first has winding numbers (n_i, m_i) and the second has winding numbers (\hat{n}_i, \hat{m}_i) , then the intersection number between the branes is

$$I = \prod_i (n_i \hat{m}_i - \hat{n}_i m_i). \quad (3.3)$$

Because of the orientifold, there is a distinction between **A** and **B** type branes a, b , which have images $a' \neq a$ and $b' \neq b$ under the action of Ω , and a **C** type brane c , which is taken to itself under the action of Ω . Given two **A**-type branes a, \hat{a} , for example, the intersection numbers $I_{a\hat{a}}$ and $I_{a\hat{a}'}$ are distinct, and must be computed separately.

3.1 Single intersection numbers

A coarse characterization of the distribution of individual intersection numbers can be given by considering the standard deviation of the set of intersection numbers within a given ensemble of pairs of branes. In the absence of negative tadpoles, we might expect that typical winding numbers would be of order $T^{1/3}$, giving typical intersection numbers of order T^2 . Even for type **B** branes, however, this is not quite right. Generally the winding numbers are not evenly distributed. For example, from the analysis leading to (2.24), we see immediately that at least order T^2 of the $T^2(\ln T)^2$ type **B** branes undersaturating all tadpoles have three winding numbers (*e.g.* m_i) of order 1, and two winding numbers (*e.g.* n_2, n_3) of order T . Thus, there are at least order T^4 **BB** combinations of the form $n \sim (0, T, T), m \sim (1, 1, 1), \hat{n} \sim (1, 1, 1), \hat{m} \sim (0, T, T)$ which have $I_{b\hat{b}} \sim T^4$. It is also easy to show that a **BB** intersection number cannot be larger than $8T^4$, so we expect the rate of growth of the standard deviation in this ensemble to be order T^4 up to logs. Because of the negative tadpoles on type **A** branes, which allow branes to have larger winding numbers, we expect a broader distribution of intersection numbers for fixed T when other brane types are considered. For example, in an **AB** configuration with a hidden sector **A** brane, we can have **A** brane winding numbers which go as $n \sim (T^3, T, -T), m \sim (1, 1, -1)$ and **B** brane winding numbers which go as $\hat{n} \sim (1, T^3, 1), \hat{m} \sim (0, 1, -T)$. This would lead to a reasonably generic class of configurations with intersection numbers going as T^7 . We have not found any configurations which would have faster growth, so we expect the standard deviation of intersection numbers of pairs of branes to grow polynomially in T , with a rate of growth somewhere between T^4 and T^7 .

We have computed the intersection numbers for all brane combinations of each type (assuming no hidden sector **A** branes) at various values of T . The standard deviations of the resulting distributions are plotted in Figure 4. We see that indeed the overall standard deviation grows faster than T^4 ; the growth is dominated by **AB** configurations, which in the absence of hidden sector **A** branes have intersection numbers which grow as T^5 from configurations with, for example, $n \sim (T, T, -T), m \sim (1, 1, -1)$ and $\hat{n} \sim (1, 1, T^3), \hat{m} \sim (0, T, -1)$. The intersection numbers are generally much smaller for

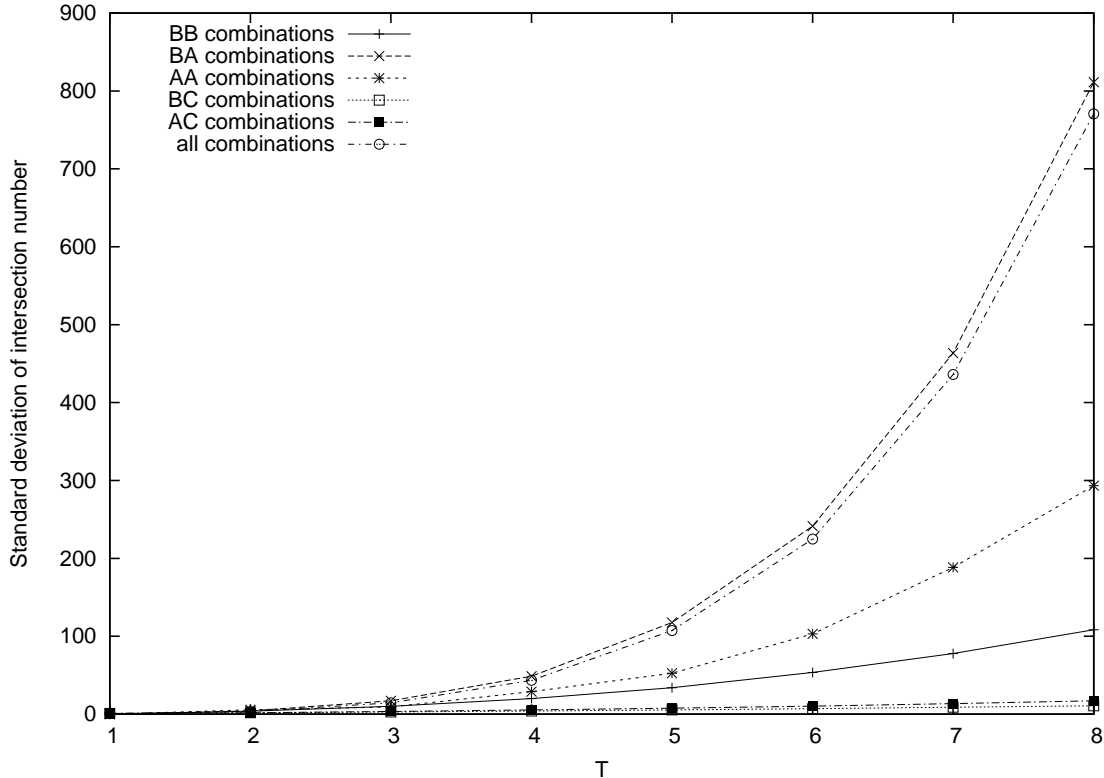


Figure 4: Standard deviation in intersection number for different brane combinations

combinations containing type **C** branes, as all nonzero winding numbers for type **C** branes are 1.

The entropy H of the distribution of intersection numbers characterizes the amount of information needed to fix a single intersection number. For a reasonably smooth distribution, generic values will appear with frequency roughly 2^{-H} . We have computed the entropies of the distributions of intersection numbers for different types of branes, which are plotted in Figure 5. The entropies grow roughly as the log base 2 of the standard deviations, indicating a reasonably uniform distribution.

While we have computed the intersection numbers for generic T assuming that we are combining single branes, we can also interpret these results in terms of intersection numbers when the size N of the brane stacks is increased. For example, in Figures 4, 5 the intersection numbers for a given value of T are equal to those for the desired physical

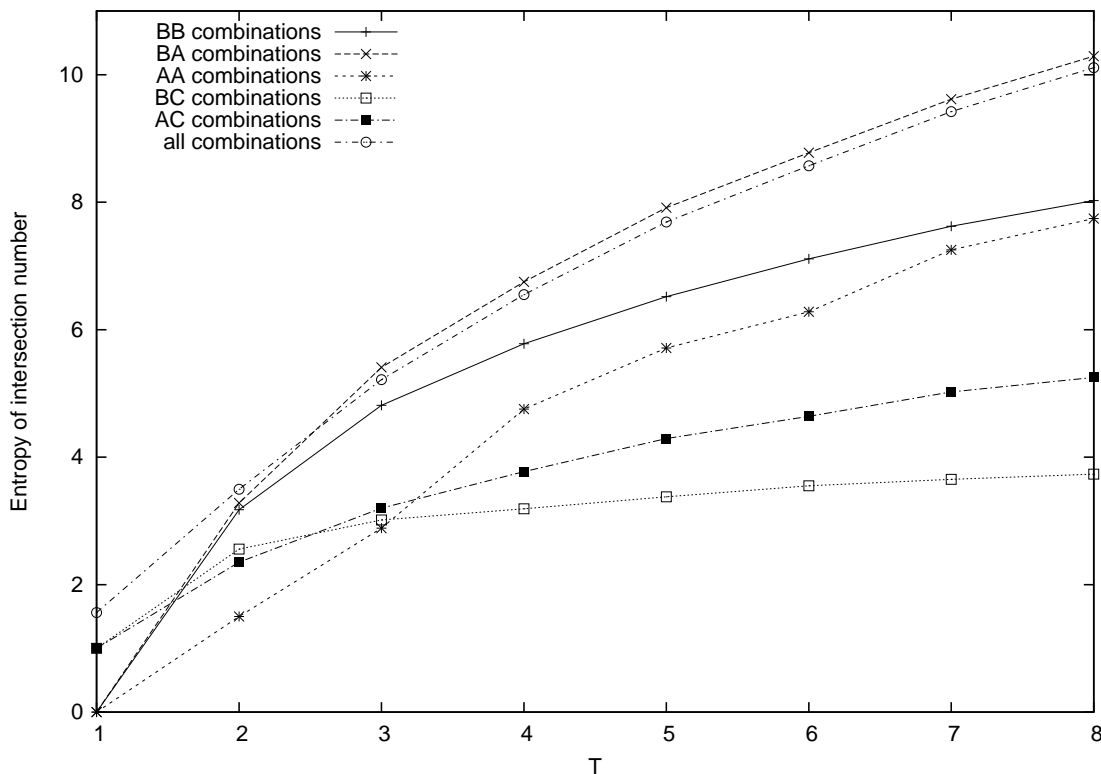


Figure 5: Entropies in intersection numbers for different brane combinations

tadpole value $T_0 = 8$ and brane stacks of size $N = 8/T$. For example, for single **A**, **B** branes with $T = 4$ the intersection number has a standard deviation of ~ 50 . This is the same as for a pair of brane stacks each with $N = 2$ with $T = 8$. The consequence of this is that for larger gauge groups, the intersection number is polynomially suppressed. While for a $U(1) \times U(1)$ theory, typical intersection numbers are in the hundreds (assuming hidden A branes are not included; including such branes would leave to even larger intersection numbers), when even a gauge group like $U(2) \times U(2)$ is included the intersection numbers are reduced by a numerical factor of order $2^5 = 32$ (the factor in the data graphed in Figure 4 is slightly smaller than this, presumably due to log suppression of the rate of growth). When the gauge group has several factors of different rank, it is difficult to give a precise estimate for the suppression of intersection numbers, but for generic configurations including the possibility of hidden sector A branes, we expect an overall suppression by a monomial of degree around 7 in the sizes of the gauge group components. Thus, typical intersection numbers of a generic model with for example $U(4) \times U(2) \times U(2)$ will be down by a factor of at least 2^7 from intersection numbers in generic $U(1) \times U(1) \times U(1)$ configurations.

The information contained in the standard deviation and entropy of the intersection number distributions give a rough characterization of the overall structure of these distributions. A plot of the overall distribution of intersection numbers for pairs of branes at

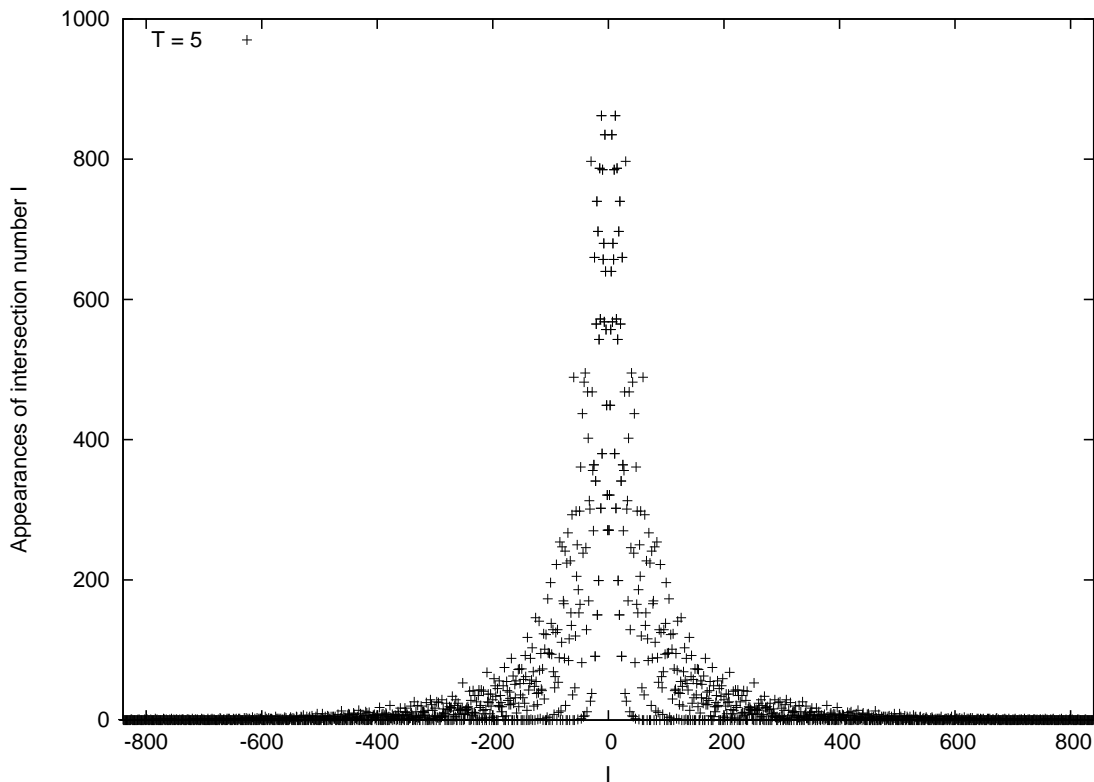


Figure 6: Frequencies of intersection numbers at $T = 5$

$T = 5$ is shown in Figure 6. As expected from Figure 4 the width of the distribution is of order 100. The distribution is fairly sharply peaked, and has some fine structure. A closer look at the detailed distribution of intersection numbers reveals some further features. In Figure 7 we plot the frequency with which individual intersection numbers take integer values from 0 to 30 at $T = 5$ and $T = 6$. The pattern shown by this plot is that composite intersection numbers with many factors are favored, and 0 is very strongly favored, while prime intersection numbers and other intersection numbers with few factors are disfavored. This feature, as well as the sharply peaked nature of the distribution, comes from the structure of the intersection number formula (3.3), which is a product of 3 terms each of the form $n\hat{m} - m\hat{n}$. While this structure is specific to the toroidal model we are considering here and presumably is not relevant for more general Calabi-Yau manifolds with more general intersection formulae, we can briefly give a quantitative explanation for the relative prevalence of different small intersection numbers. Consider for example the parity of the intersection number, associated with whether it is divisible by 2 or not. If the individual winding numbers were chosen with arbitrary parities, of the 16 possible values for the individual parities, $n\hat{m} - m\hat{n}$ has parity 0 for 10 combinations and parity 1 for 6 combinations. This would suggest that only $(6/16)^3 \approx 5\%$ of the intersection numbers should be odd. Because the winding numbers n_i, m_i are relatively prime and not evenly distributed (for example, 1 is particularly frequent), the true fraction is significantly larger.

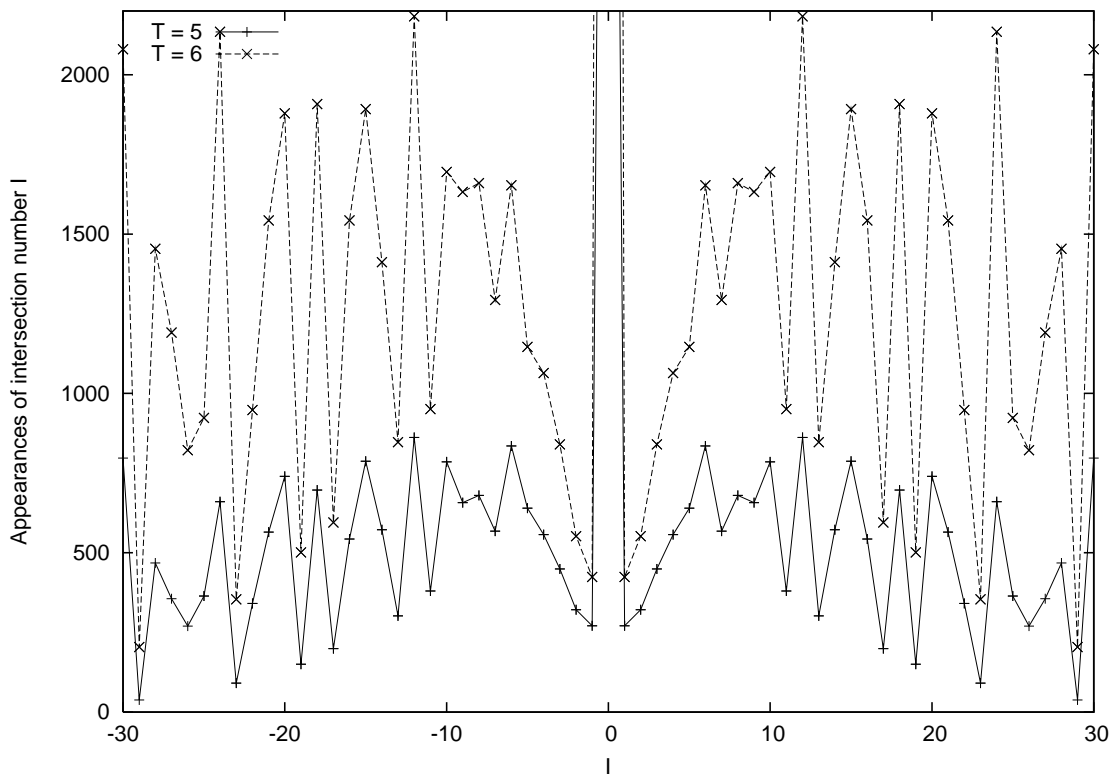


Figure 7: Frequencies of small intersection numbers

In fact, we have 30% odd intersection numbers at $T = 4$ and 33% odd intersection numbers at $T = 6$. Similarly, we generically expect intersection numbers to be congruent to $0 \pmod p$ for each p with an enhancement factor which decreases with growing p . This number theoretic suppression of intersection numbers with few factors has a noticeable but relatively mild effect on the prevalence of different intersection numbers, although it does lead to a significant enhancement of the probability for a vanishing intersection number. Among small intersection numbers it does suppress 1 more than other numbers, but considering for example the frequency of appearance of the intersection number 3 across all brane pairs, we find at $T = 6$ that the intersection number 3 appears about 0.66% of the time, which is not particularly frequent or infrequent compared to other numbers in the range from -100 to 100 , and which is quite compatible with the entropy $H \approx 8.57$ for intersection numbers of pairs of branes at $T = 6$, which suggests that typical intersection numbers will appear with frequency of order 0.5%. For comparison, the most common nonzero intersection number 12, with many factors, occurs about 1.8% of the time, while a more highly suppressed larger prime intersection number like 23 occurs about 0.27% of the time. Again, the greatest enhancement is for vanishing intersection number, which occurs 7.5% of the time.

It is also worth noting that in model building, when we consider two branes x and y which are not invariant under Ω , the number of chiral fermions will go as the sum $I_{xy} + I_{xy'}$.

This addition of intersection numbers tends in general to ameliorate somewhat the number theoretic suppression or enhancement of certain values. The story is different, however, for $p = 2$. In this case, we have

$$I_{xy} \equiv I_{xy'} \pmod{2} \Rightarrow I_{xy} + I_{xy'} \equiv 0 \pmod{2}. \quad (3.4)$$

As has been discussed in many places [9], this implies that we cannot build a 3-generation model in this orientifold with type **A** and **B**-branes alone without including some additional structure like discrete B fields which can change these parity constraints.

3.2 Multiple intersection numbers

Let us now turn to pairs of intersection numbers. We are interested in determining whether there is a strong correlation between distinct intersection numbers in a given brane configuration, or whether the intersection numbers are roughly independently distributed according to the single intersection number distribution described in the previous subsection. We consider two possible types of correlation, first between intersection numbers I_{xy} and I_{xz} in a configuration of 3 branes x, y, z , and second between intersection numbers I_{xy} and $I_{xy'}$ where y and y' are related through the orientifold action Ω .

As an example of the first type of correlation, consider the most prevalent 3 brane combination **ABB** (in the absence of hidden A branes). Let us consider the ensemble of all such brane combinations $a + b + \hat{b}$. The distribution of allowed values of $(I_{ab}, I_{a\hat{b}})$ is shown in Figure 8 for $T = 3$. There are 1594 distinct **ABB** combinations for this value of T , and we consider all pairs of intersection numbers where for each brane we take either orientifold image. Including either ordering of the branes b, \hat{b} gives $16 \times 1594 = 25504$ pairs of intersection numbers. We find that the resulting distribution is very close to a product distribution. Like the individual intersection numbers considered above, combinations where either intersection number is prime are suppressed, and composite intersection numbers with many factors are enhanced. To quantify the correlations between the two intersection numbers, we have computed the mutual entropy between the distributions of the two intersection numbers. The distribution of the individual intersection numbers has entropy $H(I(x, y)) = H(I(x, z)) \approx 4.553$, while the mutual entropy is just

$$\mathcal{I}(I(x, y), I(x, z)) \approx 0.085 \quad (3.5)$$

Thus, the distributions are almost completely independent. We have not done a thoroughly comprehensive analysis of all brane configurations, but we have looked at a number of other cases and variations of this calculation, and the results appear to be fairly general. For example, for the same ensemble, the mutual information between the **AB** and **BB** intersection numbers is $\mathcal{I}(I(x, y), I(y, z)) \approx 0.102$ while the entropy of the BB intersection numbers is $H(I(y, z)) \approx 4.401$. As we increase T , the ratio of mutual information to total information decreases further.

We have also looked at the correlation between intersection numbers $I(x, y)$ and $I(x, y')$ where y, y' are related by Ω . In this case the correlations are somewhat stronger. From (3.4), the parities of these intersection numbers must be the same. There are also further

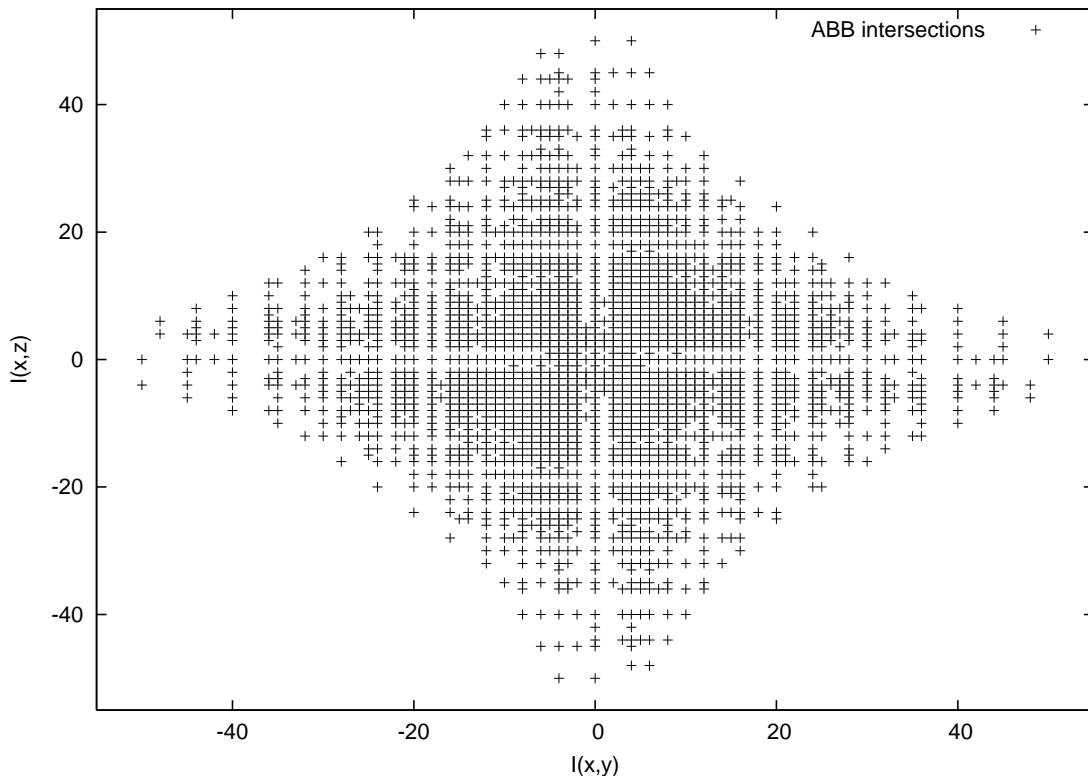


Figure 8: Intersection numbers (I_{xy}, I_{xz}) for **ABB** combinations at $T = 3$

correlations arising from the fact that the winding numbers of y and y' are the same up to signs. For the class of **AB** configurations, which dominate two-brane combinations in the absence of hidden **A** branes, we find that at $T = 4$, the entropy of each intersection number is $H(I(x, y)) \approx 6.6$, and the mutual entropy is $\mathcal{I}(I(x, y), I(x, y')) \approx 3.4$, so knowing one intersection number gives almost half the information needed to determine the other. The ratio of mutual information to total entropy decreases as T increases; at $T = 6$ we have $H \approx 8.7$ and $\mathcal{I} \approx 4.0$.

Finally, we have looked at some sets of 3 intersection numbers to see if correlations between three intersections are stronger than those between two intersection numbers. In particular, we consider again the class of **ABB** configurations without hidden sector **A** branes. In principle, we could compute the 3-way mutual entropy for the three intersection numbers. This would require a substantial amount of data for a useful test, so we have done a simpler spot test. We can select all configurations with a fixed intersection number, say $I(y, z) = I_0$ and ask whether the distribution of intersection numbers $I(x, y), I(x, z)$ is significantly different from that without the constraint on $I(y, z)$. We did this with all 49,106 **ABB** combinations at $T = 4$ for the values $I_0 = 2$ and $I_0 = 3$, which correspond respectively to 2504 and 4360 combinations. In each case we found that the distribution of intersection numbers $I(x, y), I(x, z)$ was qualitatively similar to the distribution without constraining $I(y, z)$. For example, at $I_0 = 3$, the mutual entropy was about 0.4, with

individual entropies for the **AB** intersection numbers of about 6.3. This suggests that even when 3-way correlations are considered there is very little connection between different intersection numbers.

The upshot of the analysis described in this section is that for all the brane combinations we considered here, the intersection numbers were fairly independent. For intersection numbers $I(x, y), I(x, z)$ between a fixed brane x and two other branes y, z which are not related by the orientifold symmetry and which live in an allowed combination, like the **ABB** combinations, the intersection numbers are almost completely independent. We found somewhat stronger correlations between intersection numbers $I(x, y), I(x, y')$ where y and y' are related by the orientifold action. These correlations include the fact that such pairs of intersection numbers must have the same parity, giving an even number of fermions living in this sector of the theory.

The basic conclusion which follows from this analysis is that if we wish to estimate the number of models which have a given gauge group and given numbers of chiral fermions in each matter sector corresponding to pairs of intersecting branes, we can get a good estimate by multiplying the total number of models with the desired gauge group by the product of the fractions of those models with the desired number of fermions in each sector. This provides a rough estimate of the number of models with the desired properties which can be constructed using intersecting branes in this class of orientifolds. Furthermore, we can use the algorithms described in the previous section to explicitly enumerate the desired intersecting brane configurations. By imposing the intersection number conditions as we include branes, we can produce an algorithm which enumerates all desired brane configurations with given intersection numbers in a time which scales roughly as the number of solutions, with possibly a small polynomial overhead.

4. Some specific models

We now have estimates for the number of models which can be constructed containing a particular gauge group, and we have analyzed the general structure of the distributions of intersection numbers. We have an upper bound for the number of models possible with a fixed gauge group such as $SU(3) \times SU(2) \times U(1)$ or $SU(4) \times SU(2) \times SU(2)$ which is of order $\mathcal{O}(T^{13}/N_1^2 N_2^2 N_3^9)$, with N_3 the size of the smallest factor and $T = 8$. Thus, we expect at most order 10^{10} or so configurations containing the gauge group $SU(3) \times SU(2) \times U(1)$, and order 10^7 configurations containing the gauge group $SU(4) \times SU(2) \times SU(2)$. The precise numbers of these configurations can be computed efficiently in a time of order of the number of configurations using the algorithms discussed in Section 2.7, and the resulting configurations can be tabulated. From the analysis of Section 3, we know that the intersection numbers are roughly independently distributed, with each intersection number having values typically of order $(T/N)^7$, and with some mild suppression of prime intersection numbers and enhancement of intersection numbers with many factors. Fixing 3 independent intersection numbers to take values of order 1–10, then, in a model with one of the above gauge groups, should reduce the number of models by a factor of something like 10^9 for $SU(3) \times SU(2) \times U(1)$ (using $N = 3$) or 10^6 for $SU(4) \times SU(2) \times SU(2)$ (using

$N = 4$). In either case, this leads us to expect something like order 10 models with the desired gauge group and intersection numbers.

A natural next step in this analysis might be to perform a systematic search using the methods we have described here for models with the standard model or Pati-Salam gauge group and 3 generations of chiral leptons and quarks in the appropriate representations of the gauge group. To begin to construct semi-realistic models, however, we must take into account the parity constraint (3.4), which states that $I_{xy} + I_{xy'} \in 2\mathbb{Z}$ if y is a type **A** or type **B** brane. Since the number of chiral fermions in the $U(N_x) \times \bar{U}(N_y)$ representation is given by this sum, we see that the parity constraint makes it impossible to have an odd number of generations when y is type **A** or **B**. Thus, we cannot immediately construct the expected handful of standard model-like brane configurations as discussed above, since their generations will all be even.

There are two ways in which we can evade the parity constraint and generate odd generation numbers. The first is to include discrete B fields on some of the two-tori forming the T^6 (in the T-dual picture this corresponds to skewing the tori). This approach was taken in [17, 19], where they systematically searched for constructions with the standard model or Pati-Salam gauge group and 3 generations of quarks and leptons. Because the inclusion of discrete B fields only slightly changes the equations, basically shifting the winding modes in the affected tori by $m_i \rightarrow m_i + n_i/2$, we expect that the qualitative features of the analysis we have carried out in this paper go through unchanged, so that in the presence of discrete B fields, while the parity constraint no longer rules out 3 generations, the expected number of models is still of order $\mathcal{O}(10)$. This is in nice correspondence with the results of [19], where 11 such distinct models were identified.

The second way of including odd generation numbers is to put part of the standard model or Pati-Salam group on **C**-type branes, which do not have extra image branes, and therefore are able to have odd fermion numbers. This approach was taken in [16, 50, 51, 18] where they constructed a $U(4) \times U(2) \times U(2)$ Pati-Salam model which in our language is constructed with a $U(4)$ coming from a stack of 4 **B** type branes, and two $U(2)$ factors coming from **C** type branes. The **B** type brane oversaturates a tadpole, but can be compensated by a hidden sector **A**-brane. In [48], they carried out an analysis of other hidden sector **A**-brane combinations which could also work with this construction. A similar construction of an $U(4) \times U(2) \times U(1) \times U(1)$ model was given in [14].

From the general analysis of this paper it is clear that another way to realize a 3-generation Pati-Salam model is to take the $U(4)$ to come from a stack of 4 **A**-type branes. Let us assume that we have two factors of $U(2)$ coming from **C**-type branes c and \hat{c} with tadpoles $R = 1$ and $S = 1$. From (3.3), the condition that an **A**-brane a has intersection numbers $I_{ac} = I_{a\hat{c}} = 3$ implies that

$$-n_1 m_2 n_3 = -n_1 n_2 m_3 = 3. \quad (4.1)$$

These conditions are satisfied if we take a stack of $N = 4$ **A** branes with

$$n = (3, 1, -1), \quad m = (1, 1, -1), \quad (P, Q, R, S) = (-3, 3, 1, 1). \quad (4.2)$$

along with their orientifold images with $m \rightarrow -m$. Other solutions of (4.1) are possible but require two different winding numbers to be 3, leading to more than one tadpole which is oversaturated. Taking the stack of 4 **A**-branes (4.2) and their images and the two pairs of **C** type branes, we have total contributions to the tadpole $(-12, 12, 5, 5)$. We need to include at least one additional “hidden sector” **A**-type brane to cancel the excess tadpole in Q . We have systematically searched for such hidden branes, and found 17 possibilities for this hidden sector brane, which are listed in Appendix B. There are presumably many other possible hidden sector combinations of multiple **A** branes, but we have not searched for those.

A further check which must be performed to confirm that the models we have constructed with a single hidden sector **A**-brane are allowed is to confirm that these brane combinations either satisfy the K-theory constraints (2.6) or satisfy these constraints after a further set of branes is included. Once we have a set of branes which satisfy the K-theory constraints and undersaturate all tadpoles, the brane combination can be extended to one which precisely cancels all tadpoles by adding type **C** branes, which do not contribute to the K-theory constraints (2.6). None of the 17 possible combinations listed in Appendix 2 satisfy the K-theory constraints without the addition of further branes. We have checked all 17 models for combinations which satisfy the K-theory constraints as well as the SUSY conditions with the addition of a single type **B** brane. Of the 17 models, only the 5th can be combined with a single type **B** brane to satisfy all the K-theory constraints. In this model, we start with a stack of 4 **A**-type branes as in (4.2), **C**-branes with $R = 1$ and $S = 1$, and a single **A**-type brane with

$$n = (2, 1, 3), \quad m = (1, -1 - 2), \quad (P, Q, R, S) = (6, -4, 2, 3). \quad (4.3)$$

So far this gives total tadpoles $(-6, 8, 7, 8)$. We can then add either a single **B** brane with

$$n = (14, 1, 1), \quad m = (-1, 0, 1), \quad (P, Q, R, S) = (14, 0, 1, 0) \quad (4.4)$$

which fixes all the K-theory constraints and precisely saturates all tadpoles, or we can add a single **B** brane with

$$n = (12, 1, 1), \quad m = (-1, 0, 1), \quad (P, Q, R, S) = (12, 0, 1, 0) \quad (4.5)$$

which fixes all the K-theory constraints and requires an additional pair of (really 4) type **C** branes with $P = 1$ to cancel all tadpoles.

The class of models we have constructed here are not completely realistic, in that they contain chiral exotics which are difficult to remove from the low-energy spectrum (see, *e.g.* [51, 45]). Nonetheless, they provide an illustration of how the methods we have developed can be used to construct quasi-realistic models with certain desired features. The construction described here will presumably lead to some other 3-generation Pati-Salam models if more than one hidden sector **A**-brane or more than one hidden sector **B** brane is allowed, but we have not investigated this possibility further. We content ourselves for now with this pair of new possibilities as examples of how the techniques developed in this paper allow us to systematically search for intersecting brane models with given

gauge group and numbers of chiral fermions. Like other such constructions, the models we have constructed have various “hidden sector” gauge groups and chiral matter fields transforming under the hidden gauge groups. In the UV, anomalies are cancelled by the Green-Schwarz mechanism, but in the low-energy field theory, generally these models will be anomalous, and much of the hidden sector will be lifted to a high energy scale, leaving a residual anomaly-free low-energy field theory. We leave a detailed analysis of the models we have described here for future work, our interest here is primarily as examples of the methodology developed herein and not on detailed phenomenology.

5. More general Calabi-Yau orientifolds

The type of analysis we just discussed can be directly generalized to orientifolds of other Calabi-Yau manifolds, given a sufficiently large set of supersymmetric branes. While at this point it is not clear how large a set would suffice to get a representative sample, probably the minimal requirement is to have a family with at least b^2 parameters (in IIB terms), so that the ratio between the tadpole contributions can be adjusted independently (their overall scale can be adjusted by replicating the branes). It would be nice to have a family of branes with all $2b_2 + 2$ homology classes freely adjustable. Note that for T^6/\mathbb{Z}_2^2 (leaving out fractional branes) we had 6 winding numbers while $2 + 2b_2 = 8$, so we did not quite meet this criterion even there.

In the IIA picture, the supersymmetric branes are D6-branes wrapping special Lagrangian submanifolds. The only general construction we know for these is to embed the brane in the fixed point of an antiholomorphic involution, which is not sufficiently general.

In the IIB picture, the supersymmetric branes wrap holomorphic submanifolds of the CY, and carry holomorphic bundles. Now there is a simple class of bundles we can construct on any smooth CY, namely the holomorphic line bundles. These were first suggested for model building in [5] and have been much used since. On a simply connected CY threefold, a line bundle is parameterized by its first Chern class, an element of $H^2(M, \mathbb{Z})$. Thus the line bundles provide a family of branes with b_2 parameters.

As we mentioned in subsection 2.1, on T^6 the line bundles are mirror to D6-branes with all winding numbers $n_i = 1$, so this is a natural subset of the brane configurations we considered earlier. One might ask why these simple bundles were not used in the original heterotic string constructions. The answer is that in the weak coupling and large volume limit, the supersymmetry condition Eq. (2.1) does not admit interesting solutions. We saw this implicitly in the IIB analysis above, in that solving the full conditions require finite Kähler moduli. It is also true in the heterotic string, as the μ -stability condition on bundles is exactly what one obtains by dropping the $m_1 m_2 m_3$ term from Eq. (2.1), and thus a μ -stable direct sum of line bundles would give a (non-existent) IIB brane solution in the large volume limit.

Recently in [10], it was shown that heterotic string loop effects produce a correction to the μ -stability condition which allows sums of line bundles to provide supersymmetric solutions there as well. In the $SO(32)$ string this is of the same form as Eq. (2.1) (indeed it is S-dual to it), while in the $E_8 \times E_8$ string it is similar. We mention this in passing as a

piece of evidence that all of the various known constructions are just parts of a larger (and one hopes simpler) classification.

Another natural family is the D5-branes wrapping holomorphic curves. The homology class of a curve also has b_2 parameters; of course there can be many curves in a given class so there are further discrete choices.²

In the following, we will discuss the problem of enumerating sums of line bundles and curves satisfying the tadpole cancellation conditions on general Calabi-Yau orientifolds. Let us briefly mention two other interesting sets of branes. One is the rational boundary states in Gepner models; these have been used in [31]. These correspond to certain bundles obtained by the generalized McKay correspondence for the corresponding orbifold of \mathbb{C}^5 , in a way which is discussed in [28]; the generalization of this to orientifolds is partially understood [12].

A second interesting class of branes, which makes sense for a Calabi-Yau manifold which is a subvariety of a toric variety, is the restriction of the equivariant bundles on the toric variety. This includes the large set of toric hypersurfaces, complete intersections in toric varieties, and so on, so it applies very generally. In words, we are using the fact that such a Calabi-Yau manifold admits a simple embedding into a higher dimensional space (the toric variety) with a large symmetry group (a product of $U(1)$'s); the equivariant bundles are then the bundles on which this symmetry group acts by gauge transformations. This includes the line bundles, and loosely speaking, the generalization corresponds in the case of T^6 to lifting the restriction on the winding numbers $n_i = 1$, to allow general n_i . Having said this, however, we leave further discussion of this class to future work.

5.1 General framework

We will now set up a general framework for enumerating type IIB orientifold compactifications using any set of bundles on any Calabi-Yau compactification. Another description of this class of compactifications can be found in [11]. We will assume various standard mathematical definitions and be somewhat telegraphic; it may be helpful to look ahead at the sections on the torus and on the Calabi-Yau examples.

5.1.1 Basic definitions

- M is the the Calabi-Yau threefold.
- $\mathcal{J} \cong H^{1,1}(M, \mathbb{R})$, and $J \in \mathcal{J}$ is a Kähler form. In type II theory this would be complexified by the B field, but the orientifold projection removes this continuous degree of freedom. However, there is still a discrete choice of $B = 0$ or $B = 1/2$ on each two-cycle consistent with this projection. This can be summarized in an element $2B \in H^2(M, \mathbb{Z}_2)$.
- $F \in \mathcal{F} \equiv \mathcal{J} \cap H^2(M, \mathbb{Z})$ is a normalized magnetic field strength, $F = dA$ for a $U(1)$ connection.

²In orientifold theories besides type I, it may also be possible to turn on magnetic flux F on the D5.

- By Poincaré duality, $H^2(M, \mathbb{Z}) \cong H_4(M, \mathbb{Z})$, so we can also think of this datum as the homology class of a two complex dimensional submanifold D of M . A line bundle with magnetic field F will be denoted either $\mathcal{O}(D)$ or $\mathcal{O}(F)$. Such a submanifold is called a “divisor” in algebraic geometry; a generic section of the line bundle $\mathcal{O}(D)$ will vanish on D . Physically, one can think of the D9-brane carrying such a line bundle, as a bound state of the “elementary” (zero flux) D9 with a D7 wrapped on D .
- $\{\omega^i\}$ is an integral basis for \mathcal{F} , so that a field strength can be written as $F = \sum_i f_i \omega^i$. One can also introduce an integral basis of divisors D_i .
- The dual bundle V^\vee to a bundle V is defined by inverting the transition functions. For a line bundle $\mathcal{O}(F)$, we have $\mathcal{O}(F)^\vee = \mathcal{O}(-F)$.
- If $2B$ as defined above is not zero, the field strength F which appears in all of the following definitions should be replaced by $F - B \in H^2(M, \mathbb{R})$. This can be defined by choosing a lift of $2B$ to $H^2(M, \mathbb{Z})$ and taking $(2F - 2B)/2$.
- $\mathcal{K} \equiv \bigoplus_p H^{p,p}(M, \mathbb{R}) \cap H^{2p}(M, \mathbb{Z})$ is the lattice of even homology classes. More precisely, this should be $K^0(M)$, but this matters only for the torsion, so we ignore it for now.
- Ω is the orientifold operation on a bundle. In type I theory, this is the same as the dual, thus $\Omega\mathcal{O}(F) = \mathcal{O}(-F)$. In other IIB models, Ω acts as a reflection on \mathcal{K} .
- We denote the Chern character (K theory class) of a bundle E as $[E] \in \mathcal{K}$. It is additive under direct sum. For a vector bundle E with curvature F ,

$$[E] = \text{tr } e^F.$$

For the special case of a line bundle $\mathcal{O}(F)$ this is just e^F .

- The K theoretic intersection product on \mathcal{K} is

$$\eta(K, L) = \int_M K^\vee \cdot L \cdot \hat{A}(M)$$

where $\hat{A}(M)$ is the A-roof genus as in the index formula, $\hat{A}(M) = 1 + \frac{1}{24}c_2(M)$. It is antisymmetric and integral on \mathcal{F}^2 , and determines the number of bifundamental multiplets between branes carrying the bundles K and L .

5.1.2 Calabi-Yau geometric data

So far, we have just been giving names to various standard spaces and constructions; the only dependence on M is through its second Betti number $b_2 = \dim H^2(M, \mathbb{R})$.

The non-trivial geometric data we need to know about M to construct brane theories is the following:

- $C(\alpha, \beta, \gamma) : \mathcal{J}^3 \rightarrow \mathbb{R}$ is the cubic intersection form, defined as

$$C(\alpha, \beta, \gamma) = \int_M \alpha \wedge \beta \wedge \gamma.$$

It takes integer values on \mathcal{F}^3 . Unless otherwise denoted, products on \mathcal{J} , \mathcal{F} and so on are in terms of this form.

One can equivalently think of this in Poincaré dual terms as $C(D_i, D_j, D_k)$, the number of points in which three divisors intersect. From this point of view, one can see that $C(D_i, D_j, D_k) \geq 0$ for three distinct holomorphic submanifolds.

- The second Chern class $c_2(M) \in H^4(M, \mathbb{Z})$. This is Poincaré dual to a class in $H_2(M, \mathbb{Z})$, and an equivalent way to give this information is the set of intersection numbers $c_2(M) \cdot D_i$ for a basis of divisors.
- The Kähler cone $KC(M) \subset H^2(M, \mathbb{R})$ is the set of Kähler forms of sensible Kähler metrics (all integrals $\int \omega^k$ over holomorphic cycles are positive). It is convex, *i.e.* given any $\omega_1, \omega_2 \in KC(M)$, we have $\omega_1 + \omega_2 \in KC(M)$.
- The Mori cone $MC(M) \subset H_2(M, \mathbb{Z})$ given by the effective classes; *i.e.* the classes of holomorphic curves in M . By Poincaré duality we can identify it with a subset of $H^4(M, \mathbb{Z})$. It is also a convex cone.

It turns out that the Kähler cone and the Mori cone are dual, in the sense that $\omega \in H^2(M, \mathbb{R})$ is in the Kähler cone if

$$\eta(\omega, C) > 0 \quad \forall C \in MC.$$

Thus either can be deduced from the other.

This data is used as follows. We choose a set of branes B_α , and consider a configuration

$$B = \sum_{\alpha} N_{\alpha} B_{\alpha}$$

where B_α are distinct branes and N_α are multiplicities. In type II theory this configuration would have gauge group $\prod_{\alpha} U(N_\alpha)$, before taking into account anomalous $U(1)$'s.

In a type I model, the brane configuration must satisfy

$$\Omega B = B^\vee = B,$$

and tadpole cancellation,

$$[B] \equiv T = 16 + c_2(M), \tag{5.1}$$

where “1” is the generator of $H^0(M, \mathbb{Z})$.

This is an equation between elements of \mathcal{K} , whose expansion into components is the set of tadpole constraints. To make this a bit more concrete, suppose that each of the branes

B_α is a D9-brane carrying a line bundle with divisor $D_a = \sum_i m_a^i D_i$, and comes with an image B'_α with divisor $-D_a$. Then the tadpole conditions become

$$8 = \sum_\alpha N_\alpha$$

and

$$T_i \equiv c_2(M) \cdot D_i = \sum_a N_a C(D_a, D_a, D_i)$$

where D_i runs over a basis of divisors.

For a supersymmetric compactification in the large volume limit, each brane must satisfy

$$Z_\alpha \equiv C(F_\alpha + iJ, F_\alpha + iJ, F_\alpha + iJ) = -i\lambda_\alpha \quad \lambda_\alpha \in \mathbb{R}^+$$

where $J \in H^2(M, \mathbb{R})$ is the Kähler class. The central charge Z could equivalently be written as

$$Z = \eta(e^{-iJ}, [B_i]).$$

For reasons we discuss momentarily, here we restrict attention to the large volume limit, in which these conditions can be broken into

$$0 = \text{Re}Z_\alpha = -3C(J, J, F_\alpha) + C(F_\alpha, F_\alpha, F_\alpha) \tag{5.2}$$

and

$$0 < -\text{Im}Z_\alpha = C(J, J, J) - 3C(J, F_\alpha, F_\alpha). \tag{5.3}$$

Unlike the torus, where these equations are exact, on a general Calabi-Yau they will receive world-sheet instanton corrections. By the “large volume limit” we mean the limit in which these can be dropped, which is when the volumes of all holomorphic curves are large in string units. If one goes away from the large volume limit, there are further subtleties in the discussion because supersymmetric branes are in general not branes carrying bundles but instead Π -stable objects in the derived category (see [3, 15] for a discussion of this). Since many if not most of the models obtained by the construction discussed here will stabilize Kähler moduli at the string scale, these subtleties will generally be important.

While a detailed discussion is not easy and depends on the example, a subset of models for which the large volume equations might give a reasonable description is to only allow D9-branes for which the supersymmetry conditions admit simultaneous solutions at large volume, as well as D5-branes, while forbidding D7-branes,. This is because D7-branes cannot be simultaneously supersymmetric with the others without large α' corrections, and furthermore they are known to decay into the others at string scales (again, see [3] for examples and references). Admittedly this is a hypothesis which would require some justification in examples before accepting, but based on the current knowledge we think it is reasonable to explore. Of course one can also deal with this point by restricting attention to configurations which stabilize the Kähler moduli at large volume.

The generalization of Eq. (5.1) to include D5-branes wrapping holomorphic cycles is simple; now $[B]$ is simply the class of B in $H_2(M, \mathbb{Z})$. Furthermore, at least in the large

volume limit, the D5 branes in type I theory are guaranteed to respect the same supersymmetry as the O9-plane, independent of the Kähler moduli. However, unlike the torus, this statement can get corrections from world-sheet instantons. An interesting concrete example using these in which the subtleties we mentioned are addressed is [29], in which these corrections are used to break supersymmetry.

5.1.3 Matter content

Given a consistent configuration, we can study the matter content. Open strings stretched between branes give rise to matter in a variety of two-index tensor representations constructed from the fundamental E_i and antifundamental \bar{E}_i . According to the index theorem, the total matter content is

$$\begin{aligned} E_{ij} &\equiv E_i \otimes \bar{E}_j & \eta(B_i, B_j) \\ P_{ij} &\equiv E_i \otimes E_j & \eta(B_i, \Omega B_j) \\ S_i &\equiv \text{Sym}^2 E_i & \frac{1}{2} (\eta(B_i, \Omega B_i) - \eta([\Omega], B_i)) \\ A_i &\equiv \wedge^2 E_i & \frac{1}{2} (\eta(B_i, \Omega B_i) + \eta([\Omega], B_i)) \end{aligned}$$

where $[\Omega] = 1 + \dots$ is the class of the orientifold plane.

This spectrum can be usefully summarized in the generalized intersection matrix

$$\hat{I}(B_i, B_j) = \eta(B_i, B_j) + \eta(B_i, \Omega B_j).$$

The two terms are antisymmetric and symmetric matrices respectively, so this does not lose information.

5.2 Examples

5.2.1 Torus

Explicit formulas for the \mathbb{Z}_2^2 invariant subsector of T^6 :

- $\mathcal{J} \cong \mathbb{R}^3$ with integral basis $\omega_i \equiv dz^i \wedge d\bar{z}^i / 2i \text{Im}\tau_i$. The intersection form is the totally symmetric form with

$$C(\omega_1, \omega_2, \omega_3) = 1$$

and all other entries zero. Equivalently, $c_{123} \equiv 1$ etc.

- $\mathcal{K} \cong \mathbb{Z}^8$, and is the algebra over the integers generated by three *commuting* variables $\omega_1, \omega_2, \omega_3$ each satisfying $\omega_i^2 = 0$. Defining $\omega_i^\vee = -\omega_i$ and $\int a$ as the coefficient of $\omega_1 \omega_2 \omega_3$, we have

$$\eta(K, L) = \int K^\vee \cdot L.$$

In components, we write a vector

$$K = (r, \vec{f}, \vec{m}, c)$$

and the intersection form is then

$$\eta(K, K') = rc' - cr' + \vec{f} \cdot \vec{m}' - \vec{f}' \cdot \vec{m}.$$

- The orientifold operation takes $F \rightarrow -F$ and thus

$$K = (r, \vec{f}, \vec{m}, c) \rightarrow \Omega K = (r, -\vec{f}, \vec{m}, -c).$$

- A line bundle is characterized by $F = \sum_i m^i \omega_i$ with $m_i \in \mathbb{Z}$. Its Chern character is

$$[e^F] = (1, m^i, \frac{1}{2} c_{ijk} m^j m^k, \frac{1}{6} c_{ijk} m^i m^j m^k)$$

with integer entries.

This corresponds to the subset of the branes we were using earlier with all $n_i = 1$. Let us see what the rest of the branes look like. First, the other **C**-type branes with two $n_i = 0$ are clearly D5-branes wrapping the T^2 with $n_i = 1$.

On T^2 , there is a unique $U(n)$ bundle $V_{n,m}$ with constant field strength and $c_1(V_{n,m}) = m$. It is the T-dual of a D1 brane with winding numbers (n, m) . Thus the T-dual of a D6-brane in IIA theory is the tensor product bundle

$$V_{\vec{n}, \vec{m}} = \otimes_i V_{n_i, m_i}$$

with rank $n_1 n_2 n_3$. Its Chern character is the tensor product of the three sets of winding numbers,

$$[V_{\vec{n}, \vec{m}}] = \otimes_{i=1}^3 \begin{pmatrix} m_i \\ n_i \end{pmatrix}.$$

This accounts for all the **A**-type branes, and the **B**-branes with all $n_i \neq 0$. The **B**-branes with one $n_i = 0$ are D7-branes carrying bundles in IIB terms. As we discussed earlier, on more general string-scale Calabi-Yau manifolds the large volume discussion will tend to break down for these branes.

One can check that the supersymmetry conditions agree with those we were using earlier (possibly up to signs in the definitions). To check the tadpole conditions, one needs to compute $c_2(M)$ for M a smooth resolution of $T^6/\mathbb{Z}_2 \times \mathbb{Z}_2$. This was done for a related but slightly different case (compactification with D7 and D3 branes) in [25]. There, it was found that matching the orientifold tadpole implies the presence of O3 planes in the resolved space as well as O7 planes. The standard $T^6/\mathbb{Z}_2 \times \mathbb{Z}_2$ orientifold of our previous discussion has O5 plane tadpole contributions in the IIB picture which presumably persist in a similar fashion even after the resolution. This generalization can be made for Calabi-Yau as well, but we save this for future work.

The intersection matrix between a pair of these branes is

$$I(V, V') = \prod_{i=1}^3 (n_i m'_i - m_i n'_i).$$

Furthermore,

$$I(V, \Omega V') = - \prod_{i=1}^3 (n_i m'_i + m_i n'_i).$$

The generalized intersection matrix is

$$\hat{I}_{ij} = \int [B_i^\vee] \cdot ([B_j] + [\Omega B_j])$$

We have

$$\hat{I}(K, K') = -2(cr' + \vec{f}' \cdot \vec{m})$$

The overall coefficient 2 here is correct and thus if \hat{I} has any odd entries, we are forced to turn on B field.

5.2.2 Elliptically fibered Calabi-Yau manifolds

Let us give another simple example³ with $b_2 = 3$, the elliptic fibration over $F_0 = P^1 \times P^1$. Let D_1 and D_2 be the divisors which are the elliptic fibrations over the two P^1 's in the base, and let the third divisor be $D_0 = B + 2D_1 + 2D_2$, where B is the section of the elliptic fibration. Then, the nonzero intersection numbers are

$$D_0^3 = 8, \quad D_0^2 D_1 = D_0^2 D_2 = 2, \quad D_0 D_1 D_2 = 1.$$

Taking the Kähler class to be

$$J = \sum_{i=0,1,2} j_i D_i,$$

the volume of the Calabi-Yau is

$$\text{vol} = \frac{1}{6} J^3 = \frac{4}{3} j_0^3 + j_0^2 j_1 + j_0^2 j_2 + j_0 j_1 j_2.$$

For a consistent metric, all holomorphic cycles must have positive volume; the subset of $j_i \in \mathbb{R}^3$ in which this is true is called the Kähler cone. We chose our basis of divisors so that the Kähler cone turns out to be simply the region with all (j_0, j_1, j_2) positive, but in general it is defined by a more complicated set of linear inequalities.

The intersections with $c_2(M)$ are given by:

$$c_2 B = -4, \quad c_2 D_1 = c_2 D_2 = 24$$

and thus the tadpole constraints become

$$8 = \sum_a N_a \tag{5.4}$$

$$-4 = \sum_a N_a 2m_1^a m_2^a \tag{5.5}$$

$$24 = \sum_a N_a (2(m_0^a)^2 + 2m_0^a m_2^a) \tag{5.6}$$

$$24 = \sum_a N_a (2(m_0^a)^2 + 2m_0^a m_1^a) \tag{5.7}$$

³We thank Bogdan Florea for providing this example.

and the supersymmetry conditions become

$$3(8j_0^2 + 4j_0j_1 + 4j_0j_2 + 2j_1j_2)m_0 + 3(2j_0^2 + 2j_0j_2)m_1 + 3(2j_0^2 + 2j_0j_1)m_2 = \quad (5.8)$$

$$8m_0^3 + 6m_0^2m_1 + 6m_0^2m_2 + 6m_0m_1m_2$$

and

$$8j_0^3 + 6j_0^2j_1 + 6j_0^2j_2 + 6j_0j_1j_2 > (5.9)$$

$$3(8m_0^2 + 4m_0m_1 + 4m_0m_2 + 2m_1m_2)j^0 + 3(2m_0^2 + 2m_0m_2)j^1 + 3(2m_0^2 + 2m_0m_1)j^2.$$

We note for comparison with the torus discussion that, while naively the total tadpoles are not all positive, if we add to Eq. (5.5) some linear combination of the other equations, the total tadpoles will become positive. However one might ask what content this has and whether there is any preferred choice of basis for these equations. We will answer this question shortly.

Many other elliptic fibrations can be found in the physics literature, as they find application in F theory, in heterotic string compactification, and so on.

5.2.3 Toric hypersurface Calabi-Yau manifolds

Such a CY is defined as the zero locus of a single equation in a four-dimensional toric variety, the “ambient” space T . Such a compact toric variety is determined by a four-dimensional polytope, and the Calabi-Yau condition then reduces to the condition that the polytope be reflexive.

A complete database of such polytopes is available at [46]. There are simple combinatoric algorithms for working out $c_2(M)$, the cubic intersection form and the Kähler and Mori cones from the polytope, see for example the appendix to [23].

It will be quite interesting to scan over this database and work out the general pattern of solutions. For example, does the number of solutions grow with b_2 , as one might expect? Or do the tadpole conditions become sufficiently complicated that explicit solutions are difficult to find?

5.3 Positivity and brane classes

As in subsection 2.2, certain basic consequences of the supersymmetry and tadpole conditions can be analyzed *a priori*, leading to a division of the supersymmetric branes into three types generalizing what we had for the torus.

We start by asking what it means for contributions to the tadpole cancellation conditions Eq. (5.1) to be positive or negative. A natural definition to make is that the “positive” tadpoles are those in the Mori cone, *i.e.* $[B] = r + T$ with $r \geq 0$ and $T \in MC(M)$. This reduces to our previous definition for the torus. It is also known that

$$ch_2(M) \in MC(M)$$

from Bogomolov’s theorem applied to the tangent bundle TM . Thus, we can again try to argue that solutions to the equations Eq. (5.1) correspond to ways to decompose a positive vector into a sum of positive and “nearly positive” contributions.

For our example of a fibration over F_0 , this definition tells us to replace Eq. (5.5) with the constraint dual to the divisor $D_0 = B + 2D_1 + 2D_2$. This is a sum over the equations Eqs. 5.5, 5.6 and 5.7 with the corresponding coefficients, giving

$$92 = \sum_a N_a (2m_1^a m_2^a + 8(m_0^a)^2 + 4m_0^a m_1^a + 4m_0^a m_2^a) \quad (5.10)$$

While equivalent, the idea is that with this definition, “most” branes will make positive contributions to the right hand side. For example, all D5’s wrapping holomorphic cycles clearly will do so, by the definition of the Mori cone.

Now, unlike the torus and our example, a general Calabi-Yau manifold will typically not have any preferred homology basis in which the Kähler cone is simply defined by $J_i > 0 \forall i$. This is because the Mori cone will typically have more than b_2 generators, and one must enforce an inequality for each generator.

One can always take the basis for $H_2(M, \mathbb{Z})$ to consist of a subset of the generators of the Mori cone, and we shall do this below. In this case, the Kähler cone will be the intersection of $J_i > 0 \forall i$ with additional inequalities.

We can now proceed to divide up the supersymmetric branes.

C) One nonvanishing tadpole.

Clearly the pure D9-brane (with no flux) is a **C**-type brane. And, if we choose our basis for $H_2(M, \mathbb{Z})$ to be a subset of the generators of the Mori cone, all other vectors with a single tadpole will correspond to D5’s wrapping holomorphic curves. Thus, we have a complete set of “filler” branes, and can again argue that any configuration of **A** and **B**-branes which undersaturates the tadpoles, can be completed in a unique way to a configuration satisfying Eq. (5.1). Furthermore, as we discussed above, the **C**-branes lead to no constraints on the Kähler moduli, at least in the large volume limit.

Note that, in the typical case in which the Mori cone will have more than b_2 generators, the precise identification of which branes are the **C**-branes will depend on our choice of basis for $H_2(M, \mathbb{Z})$.

B) Branes whose tadpole contribution lies in the Mori cone:

This includes all supersymmetric D5-branes, which as before do not constrain the Kähler moduli.

It also includes a subset of the line bundles (magnetized D9-branes). By definition, the tadpole contribution for a line bundle with flux F will lie in the Mori cone if

$$C(F, F, J) \leq 0 \quad \forall J \in KC(M) \quad (5.11)$$

(the sign is correct, as can be checked for the torus; this generalizes the minus signs we introduced in Eq. (2.3)).

This is not an easy equation to satisfy, as the coefficients c_{ijk} in our preferred basis will tend to be positive. The **B**-branes on the torus are obtained by taking (say)

$F_1 > 0$, $F_2 < 0$ and $F_3 = 0$, and relying on the vanishing of all c_{ijk} with coincident indices. In other words, these are branes whose gauge fields are non-trivial in only four of the six dimensions.

To illustrate the opposite case, consider a divisor D_1 for which the only non-zero intersections are $c_{111} > 0$ (for example a local \mathbb{P}^2). Then Eq. (5.11) forces the corresponding F to be zero.

A) Branes whose tadpole contribution lies outside of the Mori cone:

This will include most line bundles. One might go on to ask if there is any sense in which their contributions to the tadpole equations Eq. (5.1) have a “single negative component” as was the case for T^6 . This seems unlikely on the face of it, but fortunately need not be the case for a finiteness argument to work.

We should say the parallel between these definitions and those we made for the torus is not complete; in particular the power law scalings discussed in subsection 2.6 would not be expected to generalize. What we do hope will generalize is the structure of the argument in section 2 that the total number of configurations satisfying Eq. (5.1) is finite. This is again clear at a single point in Kahler moduli space, since the supersymmetry condition Eq. (5.3) forces an appropriate sum of the tadpole contributions to be positive. However we would like an argument which does not use specific values of the Kähler moduli, and provides *a priori* bounds. This is an important goal for future work.

5.4 Rough estimate of number of configurations

Neglecting the supersymmetry conditions and just looking at the general structure of the tadpole conditions Eq. (5.1), there is an obvious guess for the growth of the number of brane configurations as a function of the total scale of the tadpoles T . We have to count choices of the indices m_i^a which satisfy $b_2 + 1$ simultaneous quadratic conditions. If we take these for a single brane to all to be of order m , a plausible first guess for the size of the tadpole contributions is m^2 , and thus we can take $m \sim \sqrt{T}$. Since m for a single brane has b_2 components, we can estimate

$$\hat{\mathcal{N}} \sim T^{b_2/2}$$

for a one-stack model, with possible higher power laws for multi-stack models.

This one-stack estimate would already lead to very large numbers for typical Calabi-Yau manifolds with $b_2 \sim 100$, comparable to numbers of flux vacua. Indeed, taken at face value, this estimate would be far larger than the $(2\pi L)^{b_3}/(b_3)!$ estimate of [2], as it does not have the factorial in the denominator. Fortunately, there are many possible sources of additional b_2 dependence, which could lead to such factors. In particular, in considering an explicit example in [23], it was found that the multiplicity of terms in the intersection form tends to make its value much larger (as b_2^3 in the volume form), which could lead to a sizable suppression of the number, say to $(T/b_2^2)^{b_2/2}$. It will be interesting to get a better handle on this.

6. Relevance for the problem of counting more general vacua

Intersecting brane models are usually thought of as a special class of constructions, useful for providing concrete examples, but not necessarily mapping out the full set of possibilities; indeed one might think they are a very small subset.

A contrary intuition comes from the realization that almost all supersymmetric intersecting brane models contain many massless scalar fields, coming from open strings stretched between pairs of branes. Giving expectation values to these fields breaks part of the four-dimensional gauge symmetry, and allows moving out into a larger moduli space of configurations. One might optimistically hope that the general brane configuration could be obtained in this way.

Realizing this goal in practice requires a good deal of technical control, in particular it requires knowing the world-volume superpotential. While this has been done for some noncompact Calabi-Yau's (see for example [35, 4]), for compact Calabi-Yau manifolds it remains work in progress.

However, one might imagine that since the brane configurations are special points in these moduli spaces with enhanced symmetry, knowing all of them should give us some sort of global information about the moduli space. In this section we would like to propose an idea in this direction.

What distinguishes the IBM brane configurations, is that they transform simply under the symmetries of the compactification manifold. This is clear for hyperplanes in T^6 , which admit an action of the group of translations on T^6 . In the IIB picture, the supersymmetric branes correspond to constant curvature connections on line bundles over T^6 , for which a translation acts as a gauge transformation. More generally, this condition defines the equivariant bundles, the class of branes we suggested earlier as a good IIB analog for general toric hypersurface CY's of the branes usually used in constructing IBM's.

What use can we make of this observation? Let us consider the problem of counting all of the stabilized vacua in such a theory, which are distinguished by the values of the open string moduli. To do this, we would need not just the tree level world-volume superpotential, but the full superpotential with all non-perturbative corrections. We would then count its critical points $D_i W = 0$.

As discussed in [36, 2, 37], the number of critical points of the superpotential is quasi-topological, in the following sense. One can construct an index which weights critical points with a sign, which on a compact moduli space would be the integral of a topological density,

$$\text{index} = \int_{\mathcal{M}} \det(R + \omega). \quad (6.1)$$

The same integral makes sense on a non-compact moduli space as well, and provides a good estimate for the number of vacua for a generic superpotential.

How would one compute this? Somewhat analogous problems arise in the computation of instanton amplitudes in supersymmetric gauge theory [34, 52] and in other topological field theories. In gauge theory, the k -instanton contribution to a “protected” coupling is an integral over k -instanton moduli space of a corresponding form, typically the volume form or the Euler form depending on the amount of supersymmetry.

Now, while instanton moduli spaces are complicated, the essential point which allows computing such integrals is that they and the integrands admit continuous symmetries generated by Hamiltonians, which allows the use of localization. The obvious symmetry at hand in gauge theory on Euclidean four-dimensional space is the lift of the $SO(4)$ rotational symmetry – since a rotation on a gauge field configuration takes it into an *a priori* different gauge field configuration, we get an action involving the corresponding points in moduli space. The Hamiltonian nature of the action turns out to follow from that in Euclidean space in an analogous way.

The simplest localization arguments (which sufficed for [52]) use only an abelian group action, say $U(1)^2 \subset SO(4)$. Without going into details, the simplest application of this type of argument is the Duistermaat-Heckman formula, according to which the integral over an n -dimensional space \mathcal{M}

$$\int_{\mathcal{M}} \omega^n e^{itH} = t^{-n/2} \sum_{\text{fixed points}} \frac{1}{\det S''}, \quad (6.2)$$

where H is the Hamiltonian generating the $U(1)$ symmetry, and $\det S''$ is the one-loop determinant obtained by expanding the integrand around a fixed point of the $U(1)$ action.

The point is that, in favorable cases, the integral can be reduced to a sum over contributions from the fixed points of the $U(1)$ symmetry. On the heuristic level of our discussion, one can see various reasons why this might be applicable to the problem of counting vacua. For example, we might take H itself as a model potential $V = H$. The fixed points of the isometry $\partial H = 0$ would then be exactly the “vacua” $V' = 0$ we are trying to count. We then appeal to the quasi-topological nature of Eq. (6.1), to argue that the index counting vacua is the same for a more generic choice of potential.

Now, let us return to the problem at hand, of computing the number of stabilized vacua which can be found by starting with IBM’s and varying open string moduli. As we discussed, these will be solutions of $DW = 0$ for a generic superpotential on the moduli space \mathcal{M} of holomorphic bundles (with specified Chern classes) on the Calabi-Yau manifold M . Since M is Kähler, this moduli space will be Kähler and thus symplectic. And by general arguments, the index counting critical points $DW = 0$ will be the integral of the density Eq. (6.1) over this moduli space.

Now, suppose for a moment that M admitted a continuous symmetry; then so would the moduli space \mathcal{M} . In particular, for $M = T^6$, translations will act on \mathcal{M} , and the equivariant bundles will be the fixed points. As we discussed in section 5, these are just the type IIB description of the IBM’s we have been counting.

While a more general Calabi-Yau manifold will not have continuous symmetries, if we restrict attention to the subset of bundles which restrict from an ambient toric variety, the moduli space of such bundles will again admit a continuous symmetry, and again the equivariant bundles will be the fixed points. These include sums of line bundles and thus the right hand side of a formula like Eq. (6.2) will include a sum over the IBM’s defined in section 5, as well as other IBM’s constructed using higher rank equivariant vector bundles. If these were fewer or comparable in number, and the $1/\det$ factors of order unity, the sum could be estimated by simply counting IBM’s.

The main point of these heuristic arguments is that the IBM's are not arbitrary points in moduli space, but special points which carry information about the global topology of the moduli space. While there would be many technicalities to address in trying to make such arguments precise, such as the presence of singularities, the computation of the $1/\det$ factors, and so on, they suggest that the crude estimate “number of vacua roughly equals number of IBM configurations” might be reasonable for the open string sector.

7. Conclusions

In this paper we have developed tools for systematically analyzing intersecting brane models. We have looked in detail at a particular toroidal orientifold and characterized the gauge groups and intersection numbers associated with intersecting brane models on this space.

We have proven that there are a finite number of solutions of the Diophantine equations arising from the supersymmetry constraint, so that there are a finite number of different intersecting brane constructions in this model. We have developed estimates for the number of configurations which contain a given gauge group. The number of models with a fixed gauge group scales polynomially in the tadpole constraint, and is suppressed by a factor polynomial in the sizes of the gauge group components.

We have looked at the distribution of intersection numbers which govern the number of generations of chiral matter fields charged under the gauge group living on the branes. We found that generally the intersection numbers are almost completely independently distributed, and that the expected magnitude of the intersection numbers scales as an inverse power of the size of the gauge group components. We found a mild suppression for prime intersection numbers and enhancement of composite intersection numbers with many factors.

There are several ways to use the methods we have developed here. Most concretely, one can use the estimates and algorithms we have developed to first estimate the number of models with a given desired gauge group and matter constant, and then to explicitly construct the precise set of such models compatible with SUSY and other constraints in an efficient way. This gives a systematic way to build models which agree with certain properties of the standard model, which can then be studied for further physics predictions. The standard choice of the properties to reproduce are to get a gauge group containing the standard model gauge group, three generations of matter, and two or more Higgs doublets. Additional charged matter is usually allowed, but different works differ on the rules at this point.

The $T^6/\mathbb{Z}_2 \times \mathbb{Z}_2$ orientifold we have focused on has been the focus of much work of this type and thus we can test our results against this work. Most constructions leading to three generation standard models require turning on discrete B fields, a class which we have not enumerated. However our estimates should apply to this case and suggest that there should be about ten brane constructions which give three generation Standard Models. In fact, such models were systematically constructed in [19], where 11 such models were found. Other less generic constructions using branes invariant under the orientifold action led to

3-generation Pati-Salam models with $U(4) \times U(2) \times U(2)$ gauge groups in [16, 50, 51].⁴ We found another pair of such explicit constructions here using our understanding of the range of possibilities allowed. It would be worthwhile to understand the detailed phenomenology of these models better, and to complete the search for standard model-like IBM's which can be realized in this orientifold.

Using the techniques we have developed here, it would be straightforward to automate such a search not only for the particular orientifold we have considered here, but for a general toroidal orientifold. Carrying out a similar analysis for a broader class of Calabi-Yau orientifolds involves further issues which we have begun to address here, by setting out an approach to an analog of the intersecting brane model construction for type I strings on general Calabi-Yau manifolds.

Another way to think about the analysis of this paper is as a snapshot of a piece of the full string landscape. In [8] indications were found that some features of the standard model, such as the components of the gauge group and the number of generations of different types of matter, could be dialed fairly independently. We have developed a more complete picture of the distribution of possibilities, and searched for correlations between distinct intersection numbers using the information theoretic notion of mutual entropy. The results fit with the idea that different intersection numbers are to a good approximation independently distributed, as suggested in [36] and as emerged from the detailed studies of [8, 40].

One definite correlation which does emerge is that larger rank gauge groups come with much smaller intersection numbers, according to a power law $I \sim (\text{tadpole}/\text{rank})^\alpha$ with a large exponent $\alpha \sim 7$.

Of course, this is a very small sample even of type II orientifold models, and we would suggest broadening the class of models (at least to general Calabi-Yau orientifolds) before ascribing too much significance to these results. We should also keep in mind that the simple statistical analyses we made can miss a great deal of structure. For example, anomaly cancellation fixes definite relationships between the numbers of generations of different types of matter which will be seen in the low energy theory. Since these conditions depend on the total matter content, they do not lead to simple pairwise correlations. Perhaps other, more subtle structure of this type lies buried within the data.

As many have stressed, a noteworthy general feature of IBM's is that their gauge groups tend to be larger than that of the Standard Model, leading to new dynamics (if there is matter charged under both the SM and the new gauge groups), and hidden sectors. Similar observations about heterotic string constructions, such as the presence of extra $U(1)$'s and of course the second E_8 as a hidden sector, go back to the mid-eighties (see [30] for some recent statistical work on heterotic constructions). Clearly this would seem to be the most promising area for making interesting phenomenological predictions from this type of data. As hypothetical examples, we might imagine eventually making statements such as “the vast majority of known realistic string compactifications contain one or more extra $U(1)$'s,” or contain extra matter charged under the Standard Model group, or hidden sectors with

⁴See also [43, 44] which constructed models with partial $N = 1$ supersymmetry.

cosmological implications, or something else. Admittedly, as long as realistic models exist in which such a property is not true, it would not be a “Prediction” whose non-discovery would falsify string theory. However, it would be a “prediction” that would be worth testing as we would know it fits well with string theory; indeed to the extent that other vacuum selection criteria (measure factors, anthropic selection or otherwise) turn out not to depend on a property, it seems entirely reasonable to say that a property realized in more vacua is favored by string theory. In addition, such a property might correlate with other observables; conversely its non-discovery would be of great significance in narrowing down the search for the correct vacuum.

There are many issues which must be addressed in order to make such predictions. On the more phenomenological side, of course one needs additional input besides the charged matter content to decide what part of the model is visible at accessible energies. Even the simplest case of matter which is chiral under the SM group (and thus gets its mass from electroweak symmetry breaking), while generically ruled out by existing data, is not absolutely excluded; these constraints (which do not require any string theory input) have (to our knowledge) not been spelled out completely in the literature.

On the more formal side, one has the problem that the number of possible hidden sectors for a given visible sector model is exponential in the difference between the tadpoles of the visible sector and the total tadpole number. This tends to make the problem of enumerating even the possible matter sectors arising from all string models intractable. This motivates the style of analysis we made, in which one enumerates models with the correct visible sector, and settles for estimates for the number of possible hidden sectors. However, to the extent that one must make a detailed model-by-model study to determine which models are potentially consistent extensions of the Standard Model, this is not very satisfying. To resolve this problem, we need simple and general criteria which tell us whether a model is likely to work (or what degree of tuning is required to make it work), without using detailed information.

As an example which illustrates what we have in mind, it would be very useful to have a simple criterion for a gauge sector to dynamically break supersymmetry. This has been much discussed in the literature, beginning with [1], under a “strong” definition of supersymmetry breaking which requires a theory not to have supersymmetric vacua. Another definition, which fits much better with the landscape picture, is that any sufficiently long-lived metastable supersymmetry breaking vacuum is acceptable. Since this can be accomplished by tuning the potential, one is not looking for a criterion which provides a definite “yes/no” answer, but instead tells us what fraction of the theories in a certain ensemble are expected to break supersymmetry, and with what distribution of breaking scales. This type of question was addressed for IIB flux vacua in [24]; work such as [33, 32] and especially the recent [42] suggest that the time is ripe to address this question in gauge theory.

Another important issue which we have not addressed in this paper is the interplay between the open string sector and the closed string sector, and the stabilization of moduli using fluxes. In the vacua we have considered, there are both open string and closed string moduli. Because of the open string moduli, the intersecting brane configurations we

have constructed are just isolated points in a continuous moduli space. These points are rather special points with enhanced symmetry, and as we have discussed they may give some characteristic understanding of the full moduli space, but in a complete theory we should stabilize these moduli. This will naturally occur when the closed string moduli are stabilized by the inclusion of fluxes. While some literature, such as [7, 13, 51, 21, 20], has begun to address the problem of stabilizing open string moduli in parallel with the stabilization of the closed string moduli by fluxes, a complete mathematical characterization of this problem is not yet available. The correct way to address this problem is to give a global characterization of the open string moduli space in combination with the closed string moduli space. Just as fluxes induce a superpotential on the closed string moduli space, which stabilizes the closed string moduli as in [39], the same fluxes will induce a superpotential on the open string moduli space. A local description of this superpotential on the open string moduli space was given in [41]. An important open problem is to develop a global description of this superpotential and tools for computing supersymmetric solutions of the resulting equations of motion in which both open string and closed string moduli are fixed. This would give a true characterization of a class of string vacua which could be analyzed for standard model-like properties.

Acknowledgements

We would like to thank Mirjam Cvetič, Bogdan Florea, Shamit Kachru, Gordy Kane, Robert Karp, Maximilian Kreuzer, Jason Kumar, Paul Langacker, John McGreevy, Nathan Seiberg, Steve Shenker, Gary Shiu, Eva Silverstein, Scott Thomas, Jay Wacker and James Wells for helpful conversations. We would like to thank the KITP for support and hospitality during the initial stages of this work. This research was supported in part by the National Science Foundation under Grant No. PHY99-07949. The research of MRD was partially supported by DOE grant DE-FG02-96ER40959. The research of WT was supported in part by the DOE under contract #DE-FC02-94ER40818, and in part by the Stanford Institute for Theoretical Physics (SITP). WT would also like to thank Harvard University for hospitality during part of this work.

Appendix A

In this appendix we briefly review the appearance of the ζ function when summing over relatively prime integers. The zeta function $\zeta(s)$ is defined as

$$\zeta(s) = \sum_{n=1}^{\infty} \frac{1}{n^s}. \quad (7.1)$$

This sum can be rewritten as a product over primes

$$\zeta(s) = \prod_{p \text{ prime}} \frac{1}{(1 - 1/p^s)}. \quad (7.2)$$

The Euler totient function $\phi(n)$ gives the number of integers less than n which are relatively prime to n . For a power of a prime p^k , it is easy to see that

$$\phi(p^k) = \frac{p-1}{p} p^k = (p-1)p^{k-1}. \quad (7.3)$$

Similarly, if n has distinct prime factors p_i (which may be repeated), then

$$\phi(n) = n \cdot \prod_i \frac{p_i - 1}{p_i}. \quad (7.4)$$

As a result, we have

$$\sum_n \frac{\phi(n)}{n^s} = \prod_p \left[1 + \left(\frac{p-1}{p} \right) \left(p^{-(s-1)} + p^{-2(s-1)} + \dots \right) \right] = \prod_p \left[\frac{1-p^{-s}}{1-p^{-s+1}} \right] = \frac{\zeta(s-1)}{\zeta(s)} \quad (7.5)$$

Appendix B

As discussed in section 4, we list the 17 possible hidden sector **A**-type branes which when combined with a stack of 4 **A**-type branes of the form (4.3) and C branes with $R = 1$ and $S = 1$ give a supersymmetric configuration which undersaturates all tadpoles.

$$\begin{aligned} n = (6, 1, 3), \quad m = (1, -1, -2) \quad (P, Q, R, S) &= (18, -12, 2, 3), \\ n = (5, 1, 3), \quad m = (1, -1, -2) \quad (P, Q, R, S) &= (15, -10, 2, 3), \\ n = (4, 1, 3), \quad m = (1, -1, -2) \quad (P, Q, R, S) &= (12, -8, 2, 3), \\ n = (3, 1, 3), \quad m = (1, -1, -2) \quad (P, Q, R, S) &= (9, -6, 2, 3), \\ n = (2, 1, 3), \quad m = (1, -1, -2) \quad (P, Q, R, S) &= (6, -4, 2, 3), \\ n = (6, 1, 3), \quad m = (1, -1, -1) \quad (P, Q, R, S) &= (18, -6, 1, 3), \\ n = (5, 1, 3), \quad m = (1, -1, -1) \quad (P, Q, R, S) &= (15, -5, 1, 3), \\ n = (4, 1, 3), \quad m = (1, -1, -1) \quad (P, Q, R, S) &= (12, -4, 1, 3), \\ n = (5, 2, 2), \quad m = (1, -1, -1) \quad (P, Q, R, S) &= (20, -5, 2, 2), \\ n = (4, 2, 2), \quad m = (1, -1, -1) \quad (P, Q, R, S) &= (16, -4, 2, 2), \\ n = (10, 1, 2), \quad m = (1, -1, -1) \quad (P, Q, R, S) &= (20, -10, 1, 2), \\ n = (9, 1, 2), \quad m = (1, -1, -1) \quad (P, Q, R, S) &= (18, -9, 1, 2), \\ n = (8, 1, 2), \quad m = (1, -1, -1) \quad (P, Q, R, S) &= (16, -8, 1, 2), \\ n = (7, 1, 2), \quad m = (1, -1, -1) \quad (P, Q, R, S) &= (14, -7, 1, 2), \\ n = (6, 1, 2), \quad m = (1, -1, -1) \quad (P, Q, R, S) &= (12, -6, 1, 2), \\ n = (5, 1, 2), \quad m = (1, -1, -1) \quad (P, Q, R, S) &= (10, -5, 1, 2), \\ n = (4, 1, 2), \quad m = (1, -1, -1) \quad (P, Q, R, S) &= (8, -4, 1, 2) \end{aligned} \quad (7.6)$$

References

- [1] I. Affleck, M. Dine and N. Seiberg, “Dynamical Supersymmetry Breaking In Four-Dimensions And Its Phenomenological Implications,” Nucl. Phys. B **256**, 557 (1985).
- [2] S. Ashok and M. R. Douglas, “Counting Flux Vacua,” JHEP **0401** (2004) 060 [hep-th/030704](#).
- [3] P. Aspinwall “D-Branes on Calabi-Yau Manifolds,” [hep-th/0403166](#).
- [4] P. S. Aspinwall and L. M. Fidkowski, “Superpotentials for quiver gauge theories,” [hep-th/0506041](#).
- [5] C. Bachas, “A Way to break supersymmetry,” [hep-th/9503030](#).
- [6] M. Berkooz, M. R. Douglas and R. G. Leigh, “Branes intersecting at angles,” Nucl. Phys. B **480**, 265 (1996) [hep-th/9606139](#).
- [7] R. Blumenhagen, D. Lust and T. R. Taylor, “Moduli stabilization in chiral type IIB orientifold models with fluxes,” Nucl. Phys. B **663**, 319 (2003) [hep-th/0303016](#).
- [8] R. Blumenhagen, F. Gmeiner, G. Honecker, D. Lust and T. Weigand, “The Statistics of Supersymmetric D-brane Models,” [hep-th/0411173](#).
- [9] R. Blumenhagen, M. Cvetič, P. Langacker and G. Shiu, “Toward realistic intersecting D-brane models,” Ann. Rev. Nucl. Part. Sci. **55**, 71 (2005) [hep-th/0502005](#).
- [10] R. Blumenhagen, G. Honecker and T. Weigand, “Loop-corrected compactifications of the heterotic string with line bundles,” JHEP **0506**, 020 (2005) [hep-th/0504232](#).
- [11] R. Blumenhagen, G. Honecker and T. Weigand, “Non-abelian brane worlds: The open string story,” [hep-th/0510050](#).
- [12] I. Brunner, K. Hori, K. Hosomichi and J. Walcher, “Orientifolds of Gepner models,” [hep-th/0401137](#).
- [13] J. F. G. Cascales and A. M. Uranga, “Chiral 4d $N = 1$ string vacua with D-branes and NSNS and RR fluxes,” JHEP **0305**, 011 (2003) [hep-th/0303024](#).
- [14] C. M. Chen, T. Li and D. V. Nanopoulos, “Standard-like model building on type II orientifolds,” Nucl. Phys. B **732**, 224 (2006) [hep-th/0509059](#).
- [15] *Mirror Symmetry 2*, proceedings of the 2002 CMI school, to appear.
- [16] D. Cremades, L. E. Ibanez and F. Marchesano, “Yukawa couplings in intersecting D-brane models,” JHEP **0307**, 038 (2003) [hep-th/0302105](#).
- [17] M. Cvetič, G. Shiu and A. M. Uranga, “Chiral four-dimensional $N = 1$ supersymmetric type IIA orientifolds from Nucl. Phys. B **615**, 3 (2001) [hep-th/0107166](#).
- [18] M. Cvetič, P. Langacker, T. j. Li and T. Liu, “D6-brane splitting on type IIA orientifolds,” Nucl. Phys. B **709**, 241 (2005) [hep-th/0407178](#).
- [19] M. Cvetič, T. Li and T. Liu, “Supersymmetric Pati-Salam models from intersecting D6-branes: A road to the standard model,” Nucl. Phys. B **698**, 163 (2004) [hep-th/0403061](#).
- [20] M. Cvetič, T. Li and T. Liu, “Standard-like models as type IIB flux vacua,” Phys. Rev. D **71**, 106008 (2005) [hep-th/0501041](#).

- [21] M. Cvetič and T. Liu, “Three-family supersymmetric standard models, flux compactification and moduli stabilization,” *Phys. Lett. B* **610**, 122 (2005) [hep-th/0409032](#).
- [22] F. Denef and M. R. Douglas, “Distributions of flux vacua,” *JHEP* **0405**, 072 (2004) [hep-th/0404116](#).
- [23] F. Denef, M. R. Douglas and B. Florea, “Building a better racetrack,” *JHEP* **0406**, 034 (2004) [hep-th/0404257](#).
- [24] F. Denef and M. R. Douglas, “Distributions of nonsupersymmetric flux vacua,” *JHEP* **0503**, 061 (2005) [hep-th/0411183](#).
- [25] F. Denef, M. R. Douglas, B. Florea, A. Grassi and S. Kachru, “Fixing all moduli in a simple F-theory compactification,” [arXiv:hep-th/0503124](#).
- [26] F. Denef and M. R. Douglas, “Computational complexity of the landscape. I,” [hep-th/0602072](#).
- [27] O. DeWolfe, A. Giryavets, S. Kachru and W. Taylor, “Enumerating Flux Vacua with Enhanced Symmetries,” [hep-th/0411061](#).
- [28] D. E. Diaconescu and M. R. Douglas, “D-branes on stringy Calabi-Yau manifolds,” [hep-th/0006224](#).
- [29] D. E. Diaconescu, A. Garcia-Raboso and K. Sinha, “A D-brane landscape on Calabi-Yau manifolds,” [hep-th/0602138](#).
- [30] K. R. Dienes, “Statistics on the heterotic landscape: Gauge groups and cosmological constants of four-dimensional heterotic strings,” *Phys. Rev. D* **73**, 106010 (2006) [hep-th/0602286](#).
- [31] T. P. T. Dijkstra, L. R. Huiszoon and A. N. Schellekens, “Supersymmetric standard model spectra from RCFT orientifolds,” *Nucl. Phys. B* **710**, 3 (2005) [hep-th/0411129](#).
- [32] S. Dimopoulos, G. R. Dvali, R. Rattazzi and G. F. Giudice, “Dynamical soft terms with unbroken supersymmetry,” *Nucl. Phys. B* **510**, 12 (1998) [hep-ph/9705307](#).
- [33] M. Dine, A. E. Nelson, Y. Nir and Y. Shirman, “New tools for low-energy dynamical supersymmetry breaking,” *Phys. Rev. D* **53**, 2658 (1996) [hep-ph/9507378](#).
- [34] N. Dorey, T. J. Hollowood, V. V. Khoze and M. P. Mattis, “The calculus of many instantons,” *Phys. Rept.* **371**, 231 (2002) [hep-th/0206063](#).
- [35] M. R. Douglas, B. Fiol and C. Romelsberger, “The spectrum of BPS branes on a noncompact Calabi-Yau,” *JHEP* **0509**, 057 (2005) [hep-th/0003263](#).
- [36] M. R. Douglas, The statistics of string/M theory vacua. *JHEP* **0305** (2003) 046 [hep-th/0303194](#)
- [37] M. R. Douglas, B. Shiffman and S. Zelditch, Critical points and supersymmetric vacua, submitted to *Comm. Math. Phys*, [math.CV/0402326](#).
- [38] M. R. Douglas, “Basic results in vacuum statistics,” [hep-th/0409207](#).
- [39] S. B. Giddings, S. Kachru and J. Polchinski, “Hierarchies from fluxes in string compactifications,” *Phys. Rev. D* **66**, 106006 (2002) [hep-th/0105097](#).
- [40] F. Gmeiner, R. Blumenhagen, G. Honecker, D. Lust and T. Weigand, “One in a billion: MSSM-like D-brane statistics,” *JHEP* **0601**, 004 (2006) [hep-th/0510170](#).

- [41] J. Gomis, F. Marchesano and D. Mateos, “An open string landscape,” JHEP **0511**, 021 (2005) [hep-th/0506179](#).
- [42] K. Intriligator, N. Seiberg and D. Shih, “Dynamical SUSY breaking in meta-stable vacua,” JHEP **0604**, 021 (2006) [hep-th/0602239](#).
- [43] C. Kokorelis, “GUT model hierarchies from intersecting branes,” JHEP **0208**, 018 (2002) [hep-th/0203187](#).
- [44] C. Kokorelis, “Deformed intersecting D6-brane GUTs. I,” JHEP **0211**, 027 (2002) [hep-th/0209202](#).
- [45] C. Kokorelis, “Standard model building from intersecting D-branes,” [hep-th/0410134](#).
- [46] <http://hep.itp.tuwien.ac.at/kreuzer/CY/>
- [47] J. Kumar and J. D. Wells, “Landscape cartography: A coarse survey of gauge group rank and stabilization of the proton,” [hep-th/0409218](#).
- [48] J. Kumar and J. D. Wells, “Surveying standard model flux vacua on $T^{*6}/Z(2) \times Z(2)$,” JHEP **0509**, 067 (2005) [hep-th/0506252](#).
- [49] J. Kumar and J. D. Wells, “Multi-brane recombination and standard model flux vacua,” [hep-th/0604203](#).
- [50] F. Marchesano and G. Shiu, “MSSM vacua from flux compactifications,” Phys. Rev. D **71**, 011701 (2005) [hep-th/0408059](#).
- [51] F. Marchesano and G. Shiu, “Building MSSM flux vacua,” JHEP **0411**, 041 (2004) [hep-th/0409132](#).
- [52] N. A. Nekrasov, “Seiberg-Witten prepotential from instanton counting,” Adv. Theor. Math. Phys. **7**, 831 (2004) [hep-th/0206161](#).
- [53] A. M. Uranga, “D-brane probes, RR tadpole cancellation and K-theory charge,” Nucl. Phys. B **598**, 225 (2001) [hep-th/0011048](#).